ENHANCING THE RESERVOIR UNDERSTANDING: BY IMPLEMENTING MULTI-DISCIPLINARY APPROACH TOWARDS CHARACTERIZING "THE MIANO GAS FIELD"

Munawar Shah

Mphil Geophysics

(02112111004)

Department of Earth Sciences

Quaid-e-Azam University Islamabad, Pakistan

2023

IN THE NAME OF ALLAH,
THE MOST BENEFICENT,
THE MOST MERCIFUL

CERTIFICATE

This dissertation submitted by Munawar shah is accepted in its present form by the Department of Earth Sciences, Quaid-e-Azam University, Islamabad as satisfying the requirement for the award of M.Phil. Degree in Geophysics.

RECOMMENDED BY:

DR. TAHIR AZEEM

(SUPERVISOR) _____

DR. MUMTAZ MUHAMMAD SHAH

_____

(CHAIRPERSON)

DEPARTMENT OF EARTH SCIENCES

QUAID-E-AZAM UNIVERSITY, ISLAMABAD

EXTERNAL EXAMINER _____

DEDICATION

To my parents, friends, and family. To the hard times for they taught me patience and to the good times for they taught me gratitude.

ACKNOWLEDGEMENT

First and foremost, all thanks and gratefulness are directed to Allah for all of His benevolence and blessings.

Then, I would like to express my sincere gratitude to my supervisor **Dr. Tahir Azeem** for the continuous support and guidance. His valuable and timely comments, constructive criticism and academic support contributed most in making this task easier. He not only portrayed himself as a supervisor but also a mentor.

In the end, I would like to pay gratitude to my family: my parents and siblings, and to my fellows for their everlasting love and prayers that enable me to achieve this goal. I wish them good luck and good health.

Munawar Shah

M.Phil. Scholar

TABLE OF CONTENTS

Abstract **1**

CHAPTER#01 ..... **2**

1.1 Introduction **2**

1.2 Data set: 3

1.3 Base map 3

1.4 Seismic Data Parameters: 3

1.5 Objective of research work: 5

1.6 Methodology 5

1.6.1 Seismic Interpretation 5

1.6.2 Well Logs Analysis 5

1.6.3 Well Correlation 5

1.6.4 Rock Physics Modeling: 6

1.6.5 Seismic Inversion: 6

1.7 Organization of thesis 6

CHAPTER #02 ..... **7**

2. GEOLOGY **7**

2.1 Introduction to study area 7

2.2 Structure and Tectonic Settings: 7

2.3 Stratigraphy 9

2.4 Petroleum Prospects: 11

2.4.1 Source Rocks: 11

2.4.2 Reservoir Rocks: 11

2.4.3 Cap, Seal and Trapping mechanism: 11

CHAPTER #03 ..... **12**

3. PETROPHYSICAL ANALYSIS **12**

3.1 Introduction 12

3.2 Dataset 12

3.3 Petrophysical equations 14

3.4 Basic well logs Interpretation: 15

3.4.1 Calculation of Shale Volume 16

3.4.2 Determination of Porosity 16

3.4.3 Hydrocarbon Saturation (SHC) 16

3.5 Petrophysical Results of Miano-02 16

3.6 Petro-physical results of Miano-09 well: 20
3.7 Petrophysical results of Miano-10: 23
3.8 Well Correlation 25
3.8.1. Correlation of Reservoir Zone 25
3.8.2. Spatial Variability and Thickness Changes 26
3.8.3. Base Map: 26
3.8.4. Well Positions and Distances 26
3.8.5. Variation in Thickness 26
3.8.6. Northward Thickness Increase in B-Interval: 27
3.8.7. Consistent Thickness in Reservoir Sand: 27
CHAPTER #04 29
4. SEISMIC INTERPRETATION 29
4.1 Introduction 29
4.2 Synthetic Seismic Modeling & well correlation 30
4.3 Marking and identification of seismic horizons: 31
4.4 Results 32
4.4.2 Results and Discussion: Time Contour Maps of A, B, C, and D-Intervals 34
Temporal Distribution and Sedimentation Patterns: 35
CHAPTER #05 39
5. ROCK-PHYSICS MODELLING 39
5.1 Introduction: 39
5.2 The construction of Rock physics Model 41
5.2.1 Voigt–Reuss–Hill (V–R–H) average 42
5.2.2 Self-consistent approximation (SCA) model 42
5.3 Modelling Results: 45
5.4 Cross-Plots analysis: 48
5.5 Error analysis from Cross-Plots 50
5.6 Simulation Results 52
5.7 Conclusions 54
CHAPTER #06 56
6. Seismic Inversion 56
6.1 Introduction: 56
6.2 Model Based Inversion 57
6.3 Geostatistical Stochastic Inversion (GEOSI) 60

6.3.1 Seismic Resolution 61
6.3.2 Low Frequency Model 62
6.3.3 Prior Model (SI Model) 62
6.3.4 Variogram Modelling 63
6.3.5 Wavelet 64
6.3.6 Posterior Model and Gas Sand Probability 64
6.4 Results: 65
CHAPTER #07 70
Discussions 70
Conclusions and Recommendations 71
REFERENCES 72

Abstract

Reservoir characterization is a critical aspect of hydrocarbon exploration. The Miano Gas Field located in the Middle Indus Basin of Pakistan, is well-known for its significant natural gas potential within the Lower Goru Formation. This study proposes a complete approach towards reservoir characterization that combines 3D seismic data interpretation with well logs data analysis. To achieve this, we employ Rock Physics modeling to condition well logs and apply advanced seismic inversion techniques, including Model-Based Deterministic and Geostatistical Stochastic Inversion techniques. These methods provide an enhanced understanding of the lateral continuity and spatial distribution of gas sands in the block under study. The seismic interpretation reveals the presence of a notable normal faulting structure with a prevailing NE-SW trend, while Petrophysical analysis affirms the existence of net paying gas sands within the B-Interval of the Lower Goru Formation. Furthermore, the application of advanced inversion techniques emphasizes the lateral consistency of low impedance gas sand layers, with Gaussian Simulation inversion refining our understanding of their distribution. The spatial distribution of porosity reveals areas of notable significance, particularly in proximity to the well sites where high porosity zones are observed. Conversely, in the peripheral region of the studied block, we observe relatively lower porosity values. Overall, this study shows how well seismic data and well logs can be used together to characterize a reservoir by finding the lateral distribution of producing sand layers in the B-Interval of the Lower Goru formation in the Miano block. The insights gained from this research contribute significantly to the field of hydrocarbon exploration and production by enhancing our understanding of the complex subsurface dynamics in this prolific region.

CHAPTER#01

1.1 Introduction

Miano gas field is about 62 kilometers southeast of the city of Sukkur in Pakistan's Sindh province. Approximately 42 kilometers in length, the field can be found running parallel to the strike of the strata (Figure 1.1). The Kadanwari field is around 10 kilometers distant from the southernmost well in the area, which is located approximately 45 kilometers to the southwest of the Sawan Gas field. Notably, the Mari gas and Sui gas fields, two of Pakistan's major gas fields that produce gas from Eocene-aged limestone in the Sui main formation, are located 75 and 150 kilometers to the north of this region, respectively. Both of these fields produce gas from the Sui main formation.

In order to assess the B-Sand interval of the Lower Goru Formation, which dates back to the Lower Cretaceous, a great number of wells have been drilled in the Miano field. The Miano gas field can be found in the Thar Desert, at the boundary between the Lower and Middle Indus Basins, and between the Indian basement and the Kirthar Fold and Thrust belt. Geologically speaking, this location is known as the "Indian basement." It is believed that it goes all the way back to the southern blocks.

Figure 1.1: Location Map of the study area (Abdul Fateh et. al., 1984).

1.2 Data set:

3D seismic data was used for investigating hydrocarbons potentials, which included three wells namely Miano-2, Miano-9, and Miano-10. All of the wells in the block reached depths ranging from 3,300 meters to 3,600 meters in the lower Goru "A" and "B" Sand intervals, with Miano-02 reaches A-Interval and Miano-9 and Miano-10 are drilled only up to B-Interval. Table 1.1 shows a listing of further information regarding each well separately, which includes their names, as well as their latitudes, longitudes, elevations, total depths, and statuses.

Well name	Latitude	Longitude	Kelly Bushing	Depth	HC Type
Miano-02	27.462381	69.342683	65.80	3550.0 m	GAS
Miano-09	27.483456	69.354069	64.75	3384.0 m	GAS
Miano-10	27.497239	69.358931	68.46	3418.0 m	GAS

Table 1.1 details of the wells of the study area.

1.3 Base map

A 3D seismic reflection base map provides geographic coordinates, elevation references, acquisition geometry, survey grid, line numbering, navigation data, topographic features, and coordinate systems. These factors help locate seismic data on Earth's surface, understand vertical location, and correlate seismic reflections to subsurface objects. The base map gives GPS values, establishes the survey grid, and identifies each line. Topography includes highways and waterways. The base map typically displays the positions of wells, seismic data set boundaries, orientations and shot point's locations. Figure 1.2 depicts the base map of the study area, which includes the locations of three-dimensional seismic data cube and position of three available wells for study in the study block.

1.4 Seismic Data Parameters:

The following basic parameters were in the acquisition of the seismic data

Information	Description
Polarity	SEG normal
Energy source	Dynamite (compensation filter)
Frequency content	8–80 Hz
Receiver line interval	50 m
Bin size	25×25 m
Record length	5 sec
Total fold	72
Vertical resolution	≈ 20 meters
Field Sampling Interval	2 milli second
Source line interval	350 m

Table 1.2 Seismic Data Parameters

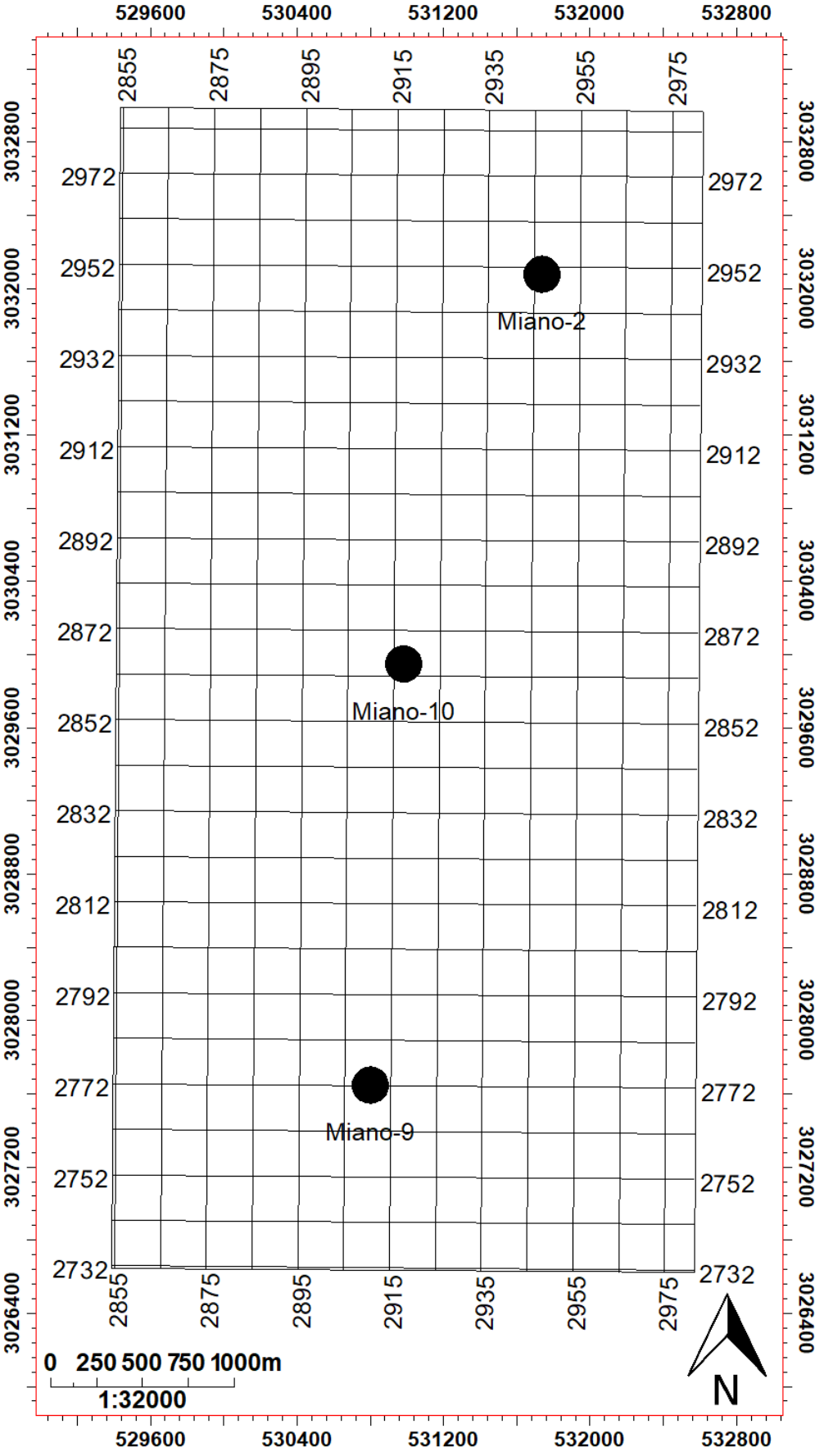

Figure 1.2: Base Map of the study area showing 3D seismic cube containing wells.

1.5 Objective of research work:

The principal objective was to delineate the subsurface reservoir's architecture and properties, encompassing the spatial arrangement of lithological units and the heterogeneity in porosity. For this purpose, following steps adopted.

- Well logs analysis to characterize the reservoir zones.
- Seismic data analysis in order to delineate the structural setting over the reservoir horizon.
- Rock-physics modelling using V–R–H average & K-T Model to estimate the elastic parameters.
- To analyze the spatial distribution of the reservoir zone within the study area. Through seismic inversion

1.6 Methodology

The methodology employed in this study involved the incorporation of the following components.

1.6.1 Seismic Interpretation

The first phase of this research involves seismic interpretation, a crucial component in the characterization of subsurface reservoirs. Seismic data acquired from various sources, including 2D and 3D seismic surveys, are employed to delineate the subsurface structure and stratigraphy. The methodology for seismic interpretation consists of the following steps:

1.6.2 Well Logs Analysis

In conjunction with seismic interpretation, well logs analysis is undertaken to provide ground truth data and to validate the results obtained from seismic data. Well data from multiple wells within the study area are collected and organized. This includes gamma-ray logs, resistivity logs, porosity logs, and other relevant well log data. The well log data are subjected to quality control procedures to identify and correct any outliers or irregularities. This ensures the reliability of the data used for subsequent analysis.

1.6.3 Well Correlation

Well correlation is a critical step in understanding the spatial distribution of reservoir properties across the study area. The methodology for well correlation consists of the following steps:

Stratigraphic Framework Development: Based on the well log data and core samples, a detailed stratigraphic framework is established. This includes identifying key stratigraphic markers and establishing the relative chronology of geological events.

Correlation Analysis: Well logs are correlated between different wells to establish lateral and vertical connections in the subsurface. This involves the identification of marker horizons and the creation of correlation panels and cross-sections.

1.6.4 Rock Physics Modeling:

Rock physics modeling is used to bridge the gap between seismic features and reservoir properties. To relate seismic features to critical reservoir factors such as porosity, lithology, and fluid content, we use known rock physics models. To understand the variability and distribution of reservoir features, statistical techniques such as statistical distributions, histograms, and cross-plots were applied to the modelled logs.

1.6.5 Seismic Inversion:

Model-based seismic inversion techniques are then applied to estimate rock properties within the subsurface. This involves the integration of rock physics models with seismic data to create high-resolution property models. Additionally, Geostatistical stochastic inversion methods are explored to account for uncertainty in the inversion results. To account for uncertainty in results, we utilize Geostatistical techniques, including variogram analysis and Kriging, to quantify the spatial variability and correlation uncertainty.

1.7 Organization of Thesis

This dissertation is structured in a manner that corresponds to the geophysical steps that are involved in characterization of reservoirs. The following chapter provides further elaboration on the geological settings of the research area, as well as the tectonic settings of the region. The third chapter is titled "Seismic Interpretation," and it comprises various different processes that are engaged in seismic interpretation. The creation of a synthetic seismogram, the calibration of a well seismogram with seismic data, the marking of horizons with intersecting faults, the production of time slices on each horizon, and, last but not least, the presentation of these horizons in a three-dimensional image are all steps that were taken in order to better understand the seismic interpretation that was carried out in the Miano area. The next stage is to conduct an examination of the elemental well logs, which may be found in the fourth chapter of this dissertation. At the very conclusion of this chapter, the Petrophysical data are presented for your perusal.

This thesis's main work is Rock-Physics modeling for reservoir interval utilizing well logs which will be discussed in next chapter. In the final chapter, seismic inversion methods are covered. These methods cover reservoir modeling using two inversion methods and their efficacy. A thesis overview with discussions and suggestions will conclude the section. This will conclude the discussion.

CHAPTER #02

2. GEOLOGY

2.1 Introduction to Study Area

This chapter covers the tectonics, structural background, stratigraphy, and surroundings of the research location in the Middle Indus basin. We will also examine how hydrocarbons shape this region's geography. Interpreting seismic data requires a good understanding of the location's tectonic geology. Because geological data underpins the study. The region under consideration is remarkable for its tectonic features and peculiar structural setting. Our inquiry will focus on tectonic components and their effects on geological formations. The study of successive information levels. Next part will reveal the region's stratigraphic makeup. To comprehend the area's geological history and progression, you must grasp stratigraphy. We will investigate both the chance of finding hydrocarbons and the relevance of the location. Hydrocarbon detection is crucial for future resource development. Finally, this chapter emphasizes the region's geological complexity and hydrocarbon potential to set a seismic data interpretation framework. This is done by summarizing the previous chapters' findings. It does this by explaining the local geology's features.

2.2 Structure and Tectonic Settings:

Tethyan and Gondwanian tectonic domains make up Pakistan, with the Indo-Pakistan crustal plate spanning the entire country. The crustal plate that runs between India and Pakistan is an important geological feature that gives Pakistan its basic architecture. Although the Indus basin is a part of the Gondwanian Domain, it displays Tethyan Domain-like geological features, especially in its more complicated northern and western parts. In terms of geology, the large basin in southeastern Pakistan that runs along the country's northeast-southwest axis stands out as the most notable feature. The Indus basin, an area of geological interest, spans over 25,000 square kilometers. According to studies (Kazmi & Jan, 1997), this tectonic zone in Pakistan is less prone to seismic activity than others in the country.

In Pakistan, the Indus basin is divided into three distinct regions: the Upper Indus basin, the Middle Indus basin, and the Southern Indus basin. The Miano Field study area is located in the Middle Indus Basin, between the Jacobabad-Khairpur and Mari Kadhkot highs. This region is the meeting point of the Central Indus Basin and the Southern Indus Basin. The uplift of the Earth's crust occurred as a result of a tectonic event near the Cretaceous-Tertiary (K-T) boundary. This uplift is significant because it marks the start of the Tertiary unconformity, a geological boundary where various faults,

both deep basement-related and shallower wrench-tectonics related, meet. A significant phase of inversion occurred in the eastern platform region of the Middle and Lower Indus basins during the late Eocene period.

The Miano block contains normal and strike-slip faults trending nearly N-NW to S-SE. These faults, similar to those in other fields nearby, have some throw and may isolate certain sand layers in the block. These Tertiary faults are most likely a consequence of crustal plate collision and subsequent rebound relief or tensional release. This inference is supported by seismic studies and fault plane solutions, which indicate their extensional characteristics. The Middle Indus basin typically features passive roof complex type structures (Kadri, 1994). For a better understanding of the regional tectonic settings of MIB refer to following Figure 2.1.

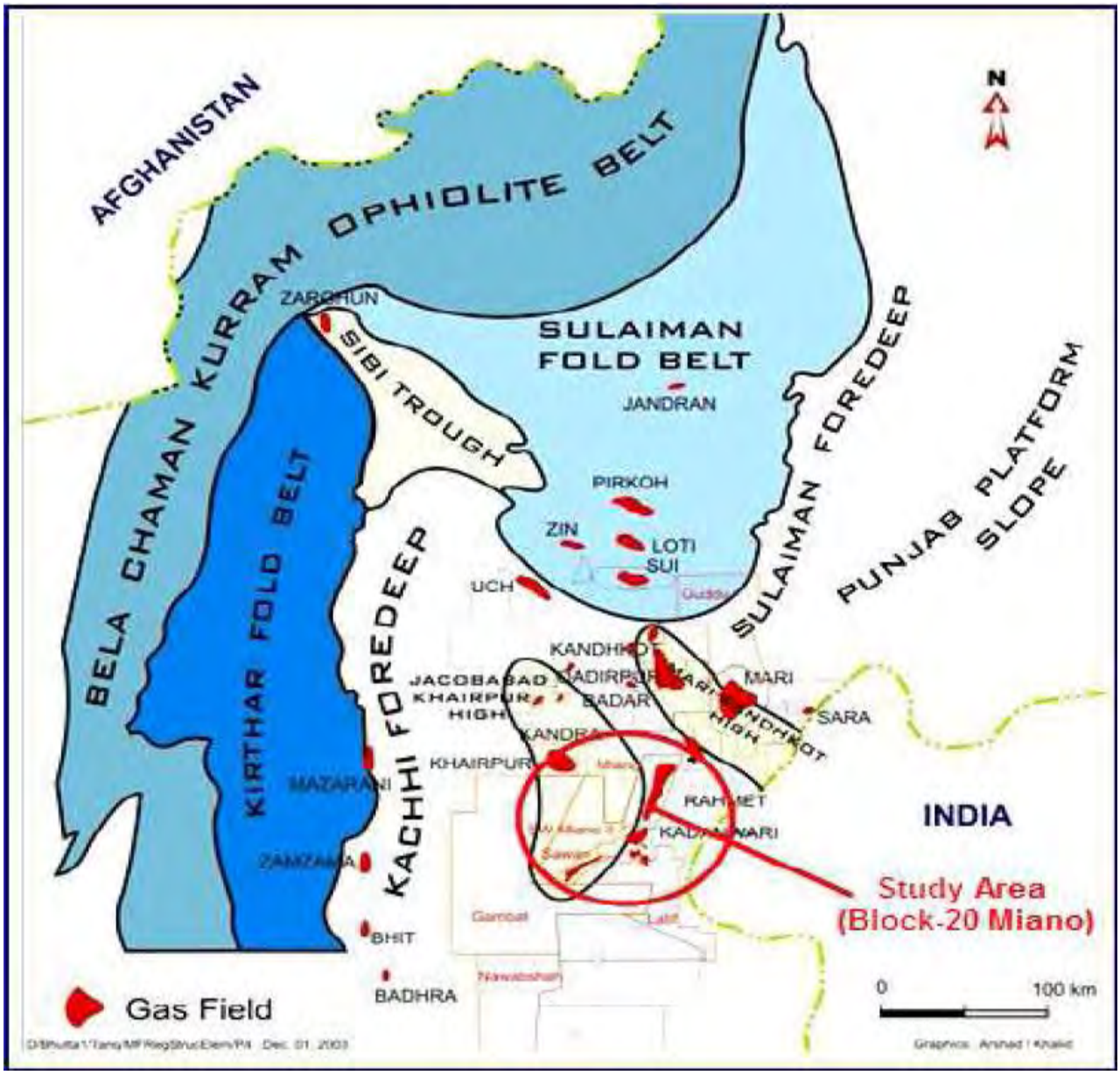

Figure 2.1: Regional tectonic map of Block-20 in the Middle Indus Basin (Mehmood et al. 2004)

2.3 Stratigraphy

The sedimentary strata found in the middle Indus basin is composed primarily of Permian to Mesozoic deposits, with a noticeable angular unconformity dating back to the late Paleozoic. The area under investigation is covered in thick alluvium strata, which obscures any direct evidence of stratigraphic sequence. The Mesozoic progradational strata are deposited on a mild eastward incline, with lateral facies fluctuation from continental to shallow marine as one moves from west to east.

Mesozoic sediments drop westward on the Thar slope and are unconformably truncated by volcanic (Khadro formation basalts) and Paleocene sedimentary rocks. Permian, Triassic, and early Jurassic sedimentary rocks are interbedded sandstone, siltstone, and shale from land or shallow marine environments.

The Middle Indus Basin may include early to middle Jurassic Chiltan Limestone. This rock is a good seismic reflector since it is smooth and flat. The reduction in Tertiary structural tilting and faulting caused by flattening seismic sections on this horizon contributes significantly to the process of elucidating depositional architecture. Overlying the Chiltan Limestone may be found regressive layers dating from the Late Jurassic to the Early Cretaceous. These strata, which include bottomsets, foresets, and topsets, prograde westward from the Indian craton.

The argillaceous foresets of the prograde, commonly known as the Sembar Formation, provide a significant portion of the basin's source rock. The topsets of the prograde are made up of the Chichali Formation and the "A" Sand Member of the Lower Goru. The sandy submarine fan systems that are linked to this progressing complex have yet to be named.

The Sembar Formation was formed when black shale was deposited in a marine environment, and it is mostly made up of black shale with trace amounts of siltstone and sandstone. It is the dominant source of hydrocarbons for the great bulk of the Lower and Middle Indus Basins, as well as the Sulaiman-Kirthar fold and thrust belt.

The Lower Goru Formation was formed at the end of a regressive system that lasted from the Late Jurassic to the Early Cretaceous. The deposition occurred during long-term eustatic or tectonic-eustatic rises in sea level of the third order, punctuated by high-frequency relative sea level fluctuations of the fourth and fifth orders. Because of these changes, prograding clastic sand packages were deposited on a massive and spreading ramp.

In addition to the westward facies-related shale-out of sands, the current eastward tilt of the strata in the research region allows for hydrocarbon stratigraphic trapping. When there is lateral (N-S) shale-out or corrosion in the reservoir quality of the "B-sand" reservoir towards the west, as well as an eastward structural tilt, a combined structural-stratigraphic trapping system is formed. Please also

Figure 2.2 for a better understanding of the simplified stratigraphic column that reflects the Indus basin.

.

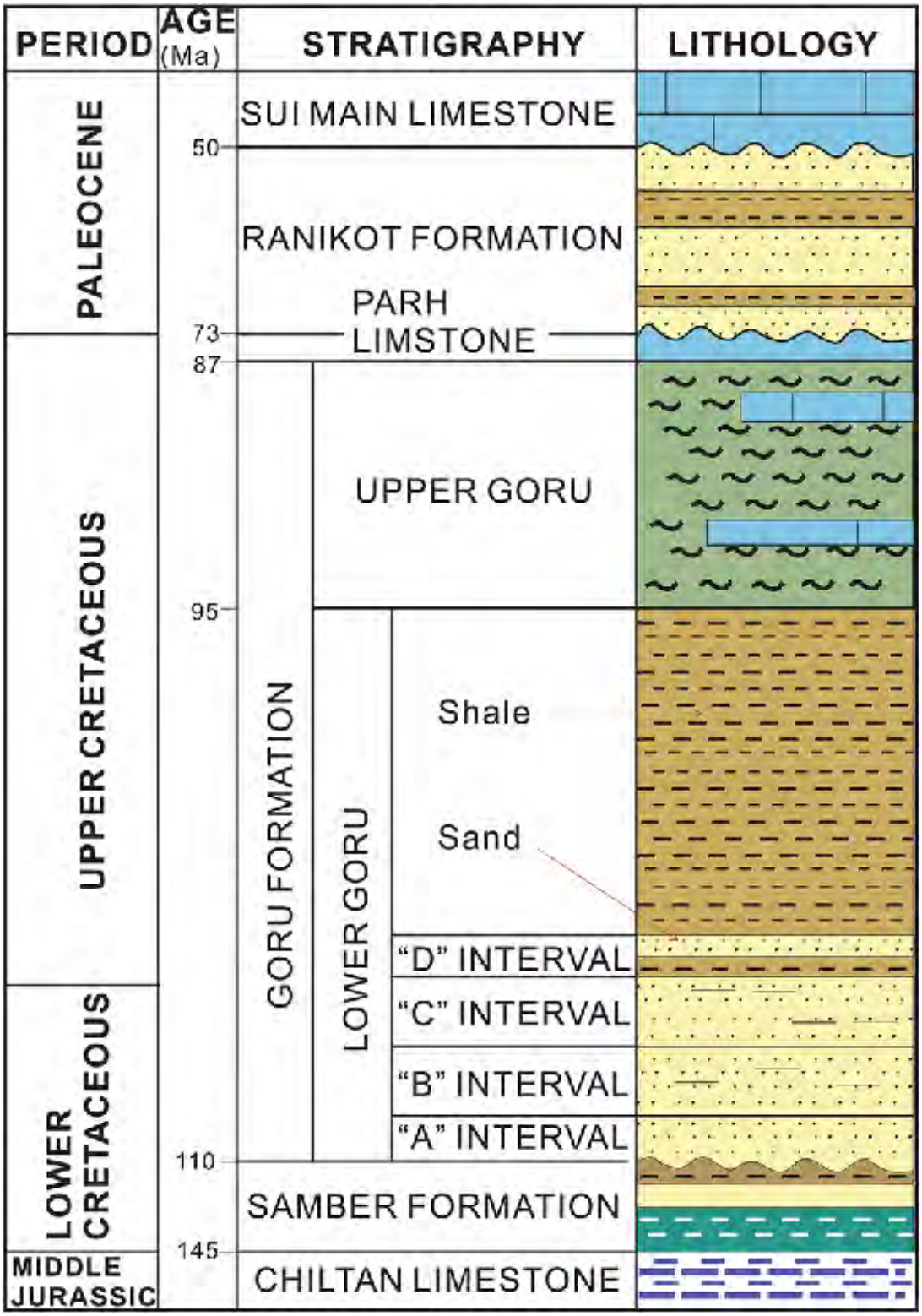

Figure 2.2: The MIB stratigraphic column with producing fields against Reservoir intervals (Azeem et al., 2017).

2.4 Petroleum Prospects:

Several gas fields are located in the research region, including Kadanwari, Sawan Miano, and Tajjal. Numerous rocks in the area's stratigraphic sequence serve as source, reservoir, and cap rocks. These are discussed under separately.

2.4.1 Source Rocks:

Source rocks are hydrocarbon-producing formations that play an important role in the conversion to organic molecules into hydrocarbons. In the research region, formations below act as the source rocks:

- The Sember Formation is an important source rock in the Indus basins, with considerable gas accumulations in the Sulaiman province. It also has reservoir potential inside its sandstone strata.
- Lower Goru shales were originally thought to be the principal source of gas in the region, as well as the source of the underlying sand deposits.

2.4.2 Reservoir Rocks:

Sands of Lower Goru Formation act as the main reservoir in the study area. These sands deposited in tide dominated environment with interbedded shales make Lower Goru formation a promising prospect. These sands are medium-hard sandstone that is yellowish-brown in color, medium-grained, and filthy white in appearance. The inter-angular porosity of these sands ranges between 10 and 15%, indicating relatively moderate levels of hydrocarbons. Both the low acoustic impedance of seismic waves and the high seismic amplitudes indicate the possibility of reservoir-quality sands. These sands, like the reservoir quality sands found in the Sawan, Miano, and Kadanwari Fields, can be found in the lowstand wedge's depositionally up-dip shallowest marine zone.

2.4.3 Cap, Seal and Trapping mechanism:

The structure and stratigraphy of the research area combine to provide a trapping mechanism for the target reservoir in this area. An isopach that trends from east to northeast to south to southwest forms the structural trap and is thick in the lower Goru "C" interval. Horsts support the isopach due to normal faulting. The trapping to the north and south west is caused by shaling out of the reservoir. The "effective zero reservoir" line is the defining feature of the northernmost limit, which is established by a facies-controlled fall in reservoir quality.

The Lower Goru Formation's thick shales and marls, together with the transgression shales of the Lower Goru "C" Interval, which are directly on top of the reservoir sands of the Lower Goru "B" Interval, combine to form the region's top seal for the reservoir. Furthermore, the shales and tight sands of the Lower Goru creation's C-Interval are responsible for the creation of lateral and bottom seals (Krois et al., 1998).

CHAPTER #03

3. PETROPHYSICAL ANALYSIS

3.1 Introduction

Petrophysics is an extremely important part of the process of characterizing reservoirs since it makes it possible to quantify and distinguish between different types of fluids. This includes shale volume, porosity, and saturation. These characteristics are necessary for precisely defining the boundaries between hydrocarbon zones. According to Daniel (2003), the integration of Petrophysics and rock physics makes it possible for geologists and geophysicists to effectively analyze both the potential benefits and the potential drawbacks of a variety of prospects. The process of accumulating data from boreholes requires geophysical well logs (Telford, 1990). These logs are sensors that measure the characteristics of the rock layers that are close to the borehole.

Using well logs data sets, the reservoirs intervals in the study region containing hydrocarbon potentials will be delineated as the primary focus of this chapter. For this purpose, data from the Miano-02, Miano-09, and Miano-10 wells were utilized. The identification of the reservoir zones was accomplished by the use of industry standard Petrophysical formulae. The analysis of quantitative well logs give vital metrics such as porosity, water saturation, lithology, and permeability, which are crucial for attaining important objectives in logging, including reservoir appraisal, well testing, and completion. It is required to take into consideration a number of important factors in order to calculate the amount of hydrocarbon reserves that are available. These factors include the lateral extent of the gas reserves, the thickness of the hydrocarbon bearing formation, the porosity of the formation, and the saturation of hydrocarbons and water within the formation.

3.2 Dataset

Research area reservoirs are characterized using Petrophysical analysis. This data is compiled from Miano wells 02, 09, and 10 boreholes. Log curves, which comprise GR (Gamma Ray), SP (Spontaneous potential), DT (Sonic log), LLD (Latro-Log Deep), LLS (Latro-Log Shallow), RHOB (Bulk density), and PEF (Photo Electric Factor), reveal important characteristics such as Vsh (volume of shale), S_w (water saturation), and SHC (Hydrocarbon Saturation (SHC)). To calculate Petrophysical properties, log types and their attributes must be distinguished. The well log tracks categorize the logs (Figure 3.1) and make them relevant and intelligible by scientists or Petrophysicists, or even a layman can understand the physical significance of logs if filled with

proper shades. This is why triple combination tracks are so common in the profession of well log interpretation.

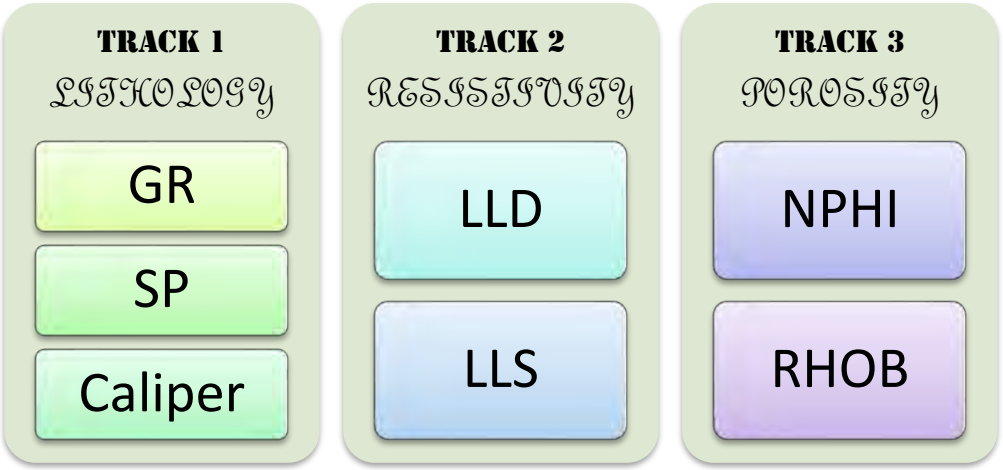

Figure 3.1: Tracks used to display and interpret well log data

The GR and SP logs are common lithology track logs. Resistivity track includes deep and shallow logs. However, the porosity track captures density and neutron porosity.

- Gamma Ray (GR) log uses gamma radiations to distinguish sand and shales based on radioactivity in formations. Asquith and Gibson (2004) state that Compton scattering is basic principal in gamma ray interaction with formations for research and lithology determination.
- Sonic Log is widely used in petroleum exploration and reservoir characterization. It works on acoustic principles. Acoustic waves are used in sonic logs to determine the interval transient time (t), which reveals rock lithology and porosity.
- Density logs records formation density using Compton scattering to determine fluid content. A study (Tittman & Wahal, 1965) found that fluid and matrix densities affect bulk density.
- A neutron porosity log estimates formation porosity in geophysics. Neutron logs also measure hydrogen content, which indicates liquid-filled porosity. Asquith and Gibson (2004) found that gas presence decreases hydrogen ion levels, reducing neutron porosity.
- The main value of electrical resistivity logs is their capacity to distinguish saline water deposits from hydrocarbon deposits. Accurate resistivity and porosity measurements are needed to calculate water saturation.
    - The LLD technique measures resistivity in undisturbed areas. This gives the device deep penetration, making it ideal for oil and gas exploration.
    - The LLS approach is crucial for determining resistivity in shallow zones, a crucial step in transition zone research.

- The Spontaneous Potential (SP) log has long been used to determine subsurface formation lithology and permeability. Low-permeability rocks like shale and clay have low electrical conductivity and spontaneous potential. Sandstone, limestone, and dolomite are highly permeable rocks that increase SP. The SP log helps locate shale, permeable formations, formation borders, water resistivity, and other formation properties.

3.3 Petrophysical equations

Geophysical logs are utilized to extract rock attributes. Several equations can be used to determine parameters such as porosity, resistivity, and saturation, as shown in **table 3.1**.

	PROPERTIES	MATHEMATICAL FARMULAE
1	VOLUME OF SHALE (VSH)	$Vsh = (\mathrm{GR} - \mathrm{GRCLN})/(\mathrm{GRSHL} - \mathrm{GRCLN})$
2	DENSITY POROSITY (PHID)	$\mathrm{PhiD} = (\mathrm{RHOMA} - \mathrm{RHOB})/(\mathrm{RHOMA} - \mathrm{RHOF})$
3	SONIC POROSITY (PORS)	$\mathrm{PORS} = (\mathrm{DLT} - \mathrm{DLTM})/(\mathrm{DLTFDLTM})$
4	TOTAL POROSITY (PHIT)	$\mathrm{PHIT} = (\mathrm{DPHI} + \mathrm{NPHI})/2.0$
5	EFFECTIVE POROSITY (PHIE)	$\mathrm{PHIE} = ((\mathrm{DPHI} + \mathrm{NPHI})/2.0) * (1 - \mathrm{VSH})$
6	PERMEABILITY	$K_e = \left(79 \times \left(\frac{\Phi^3}{S_{wirr}}\right)\right)^2$
7	RESISTIVITY OF MUD FILTRATE(RMF2)	$A = \frac{(ST + 6.77)}{(FT + 6.77)} \times R_{mfl}$
8	FORMATION TEMPRATURE (FT)	$FT = \frac{(BHT - ST)}{(TD)} \times FD$
9	SATURATION OF WATER (SW)	$SW_{\mathrm{Archie}} = \left(\frac{a}{\phi^m} . \frac{Rw}{Rt}\right)^{(1/n)}$ $SW_{\mathrm{Simandoux}} = \frac{a\,.\,Rw}{2\,.\,\phi^m}\left[\sqrt{\left(\frac{Vsh}{Rsh}\right)^2 + \frac{4\,\phi^m}{a\,.\,Rw\,.\,Rt}} - \frac{Vsh}{Rsh}\right]$ $SW_{\mathrm{Indonesia}} = \left\{\frac{\sqrt{\frac{1}{Rt}}}{\left(\frac{Vsh^{(1-0.5Vsh)}}{\sqrt{Rsh}}\right) + \sqrt{\frac{\phi_e^m}{a.Rw}}}\right\}^{(2/n)}$

Table 3.1: Petrophysical formulae used in analysis.

3.4 Basic well logs Interpretation:

The process of zone identification involves the integration of multiple logs. A low gamma ray (GR) reading is indicative of the presence of a reservoir, whilst the separation between the lower limit of detection (LLD) and the lower limit of sensitivity (LLS) and the occurrence of density-neutron crossovers serve as confirmatory evidence for the existence of hydrocarbons. The combination of parameters serves to validate the existence of productive zones.

Figure 3.2 depicts the Well log analysis work flow and the tracks for Petrophysical interpretation. Gamma ray, Spontaneous potential, Sonic, Density, and Resistivity well logs are used. Gamma ray logs reveal a rock formation's radioactivity, which is mostly due to naturally occurring uranium, thorium, and potassium. Petrophysicists deduce lithological properties from low and high radiation count rates. Density logs reveal rock formation density, making them essential in Petrophysics. This data is used to determine matrix porosity and rock minerals. Neutron logs detect neutron-hydrogen interactions in rock pore spaces to reveal rock formations' Petrophysical properties.

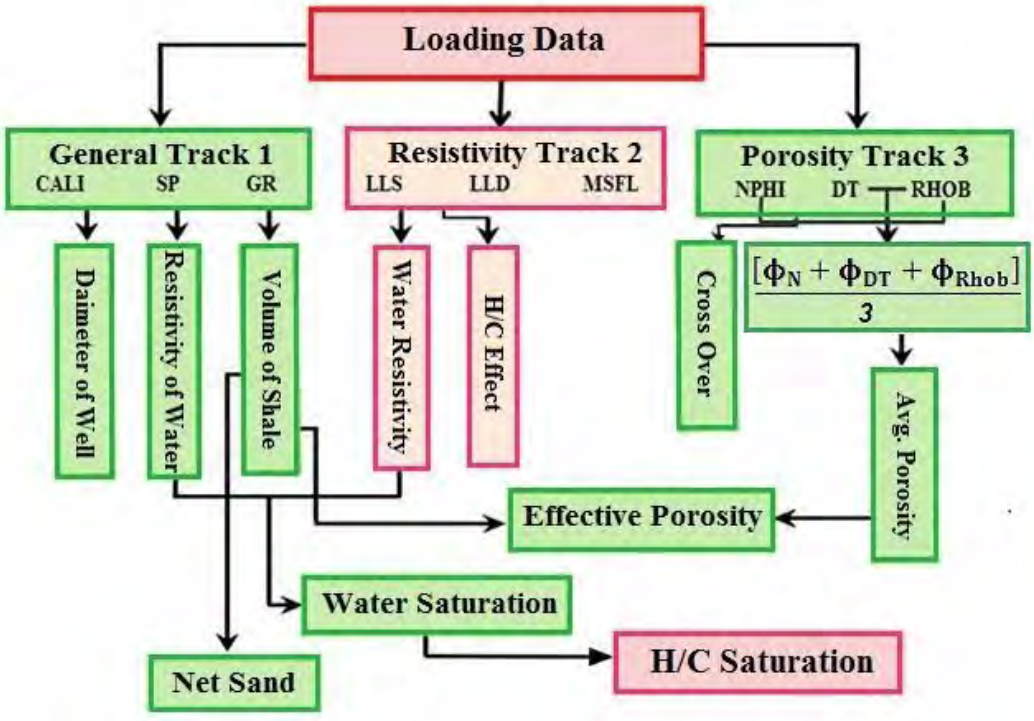

Figure 3.2: Well logs analysis workflow and tracks for interpretation purposes.

The utilization of gamma ray technology enables the identification and differentiation of shaly and sandy zones. The resistivity log provides evidence of the existence of hydrocarbons. The separation of the Latro-Log Deep (LLD) and Latro-Log Shallow (LLS) logs, the crossover of density and

neutron logs, and the support of the Gamma Ray (GR) log are all valuable tools for hydrocarbon detection.

3.4.1 Calculation of Shale Volume

The gamma ray log is utilized to measure the inherent radioactivity of geological formations, hence enabling the differentiation of lithological characteristics. A high gamma ray (GR) reading is indicative of the existence of shale, which assists in distinguishing between reservoir and non-reservoir formations.

3.4.2 Determination of Porosity

The comprehension of petroleum systems necessitates a thorough grasp of porosity, which is determined by the analysis of neutron, density, and sonic logs. The average and effective porosities are fundamental metrics.

The resistivity of formation water (Rw) is a parameter that characterizes the electrical resistance of water present in geological formations.

The process of estimating Rw entails the computation of static spontaneous potential (SSP), taking into account the formation temperature and mud resistivity as outlined in Table 3.1.

3.4.3 Hydrocarbon Saturation (SHC)

The process of calculating Hydrocarbon Saturation (SHC) involves the subtraction of water saturation from the total pore space. The equation S**HC= 1** - Sw represents the relationship between SHC, which denotes the Hydrocarbon Saturation (SHC), and Sw, which represents the saturation of water.

3.5 Petrophysical Results of Miano-02

The B interval within the Lower Goru Formation is characterized by layers composed of a mixture of shale and sand. Following geological description provides important information about the composition and lithology of the reservoir zone found in Miano -02 well as a result of Petrophysical analysis **(**Figure 3.3**).**

- Anticipated Substantial Net Income: The expectation is that this particular interval holds the potential for substantial net income. Several factors contribute to this anticipation:
- Separation between Latro-Log Deep (LLD) and Latro-Log Shallow (LLS): The Separation between the lower limit of detection (LLD) and the lower limit of quantification (LLS) is a crucial factor. This suggests that the zone contains measurable quantities of hydrocarbons, which is essential for economic viability.

- Low Gama Ray (GR): A low Gamma Ray (GR) typically indicates lower levels of natural radioactivity, which can be indicative of clean, hydrocarbon-bearing sands.
- High Resistivity: High resistivity is often associated with hydrocarbon-bearing formations, as hydrocarbons are poor conductors of electricity.
- Porosity: The presence of porosity in this zone is another positive sign, as it indicates the potential for the reservoir to hold hydrocarbons.
- Zone of Interest Extending in B and C-Intervals: The zone of interest within the Miano wells encompasses both the B and C-Intervals, with a thickness range spanning only a few meters. This suggests that the productive reservoir zone is relatively thin but contains promising properties.
- Low Shale Volume in B-Interval Sand: In the B-Interval sand portions, the shale volume is relatively low. This is advantageous as it implies that a substantial portion of this zone consists of potentially hydrocarbon-bearing sands.
- C-Interval Shale Baseline:
- In contrast, the C-Interval has a shale baseline of 60API, indicating a higher shale content in this section of the reservoir.
- High Effective Porosity in B-Interval Sand: The B-Interval sand exhibits a high effective porosity of 11.2%, which is a positive indication. Effective porosity measures the fraction of fluid-retaining empty spaces in the rock, and a high value suggests good reservoir quality.
- Hydrocarbon Potential in B-Interval Sand: The high porosity values, as well as permeability values in the B-Interval sand, indicate the potential for this zone to hold hydrocarbons, making it a promising hydrocarbon reservoir.
- Confirmation through Log Data: The confirmation of this productive zone is supported by the presence of NPHI (Neutron Porosity) and RHOB (Bulk Density) crossover and separation in resistivity logs. These logs help validate the reservoir's hydrocarbon-bearing potential.
- **Zone #1 - Highest Net Paying Zone:** Zone #1 in the Miano-02 well, as shown in Figure 3.3 & 3.3a, is identified as the highest net paying zone. It exhibits several favorable characteristics:
- High Effective Porosity and Permeability: These properties indicate good fluid retention and flow potential, making it an attractive reservoir zone.
- Low Water Saturation: Low water saturation suggests a high Hydrocarbon Saturation (SHC), making it a gas-producing zone within the B-Interval sand.

- Correlation with Other Wells: Zones from well 9 and 10 correlate to Zone-01 and exhibit almost similar properties, and confirming the presence of a productive reservoir zone in these wells.
- **Zone #2 - Moderate Reservoir Features**: Zone #2, on the other hand, has somewhat moderate reservoir features:
- High Effective Porosity and Permeability: While it has high porosity and permeability, indicating good fluid retention and flow potential, other factors make it less attractive.
- High Water Saturation: The high water saturation suggests lower Hydrocarbon Saturation (SHC).
- NPHI and RHOB Cross-Over: The small cross-over Neutron Porosity and Bulk Density indicates a less distinct separation in resistivity logs, which can be less favorable for hydrocarbon production.

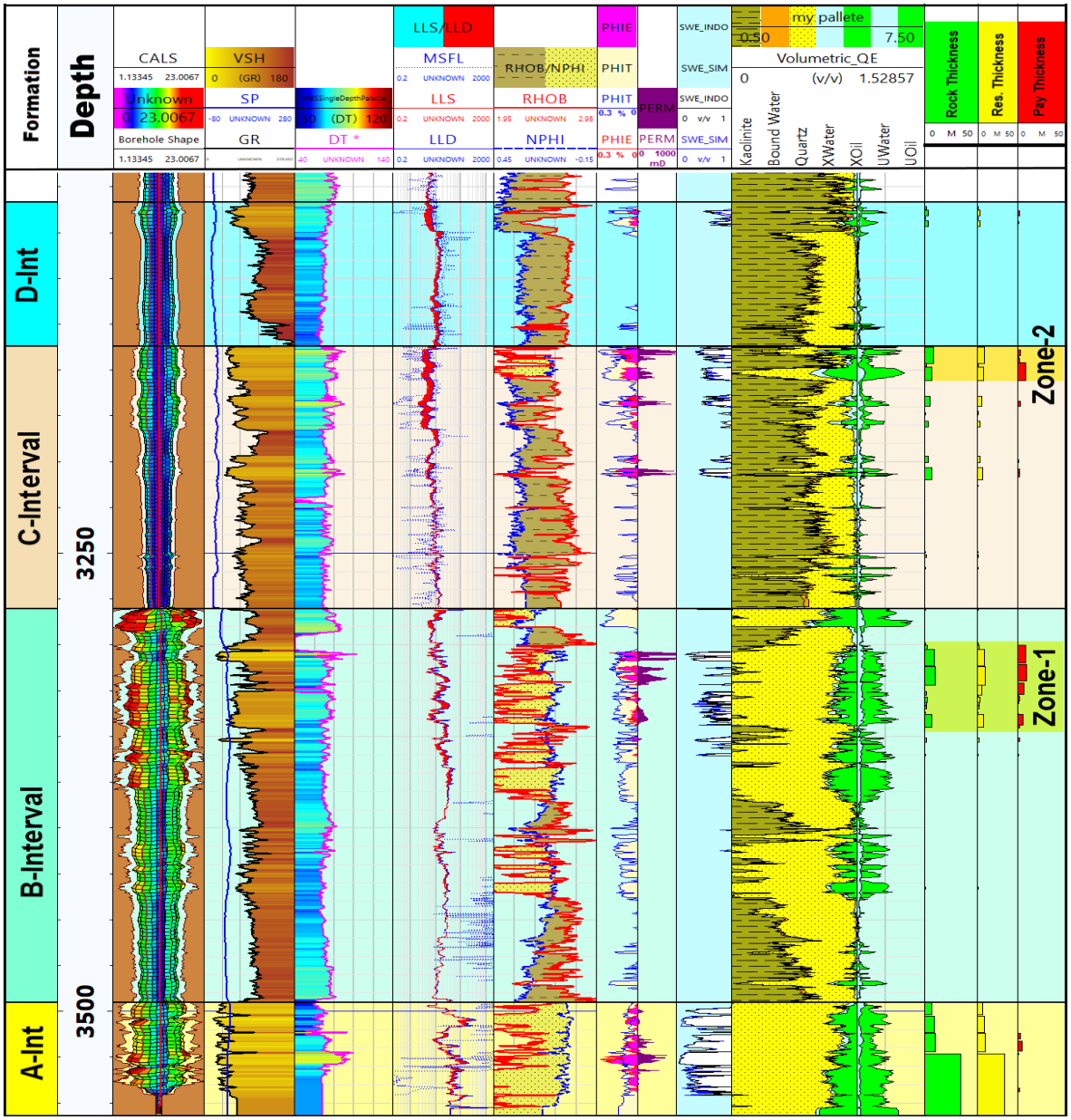

Figure 3.3: Petrophysical analysis of well Miano-02

In summary, the Miano-02 well results suggest the presence of a promising hydrocarbon reservoir zone in the B-Interval sand, particularly in Zone #1, characterized by high effective porosity, permeability, and low water saturation shown in Figure (3.3a). These findings are valuable for reservoir evaluation and development planning, with Zone #1 being the most attractive for potential hydrocarbon production.

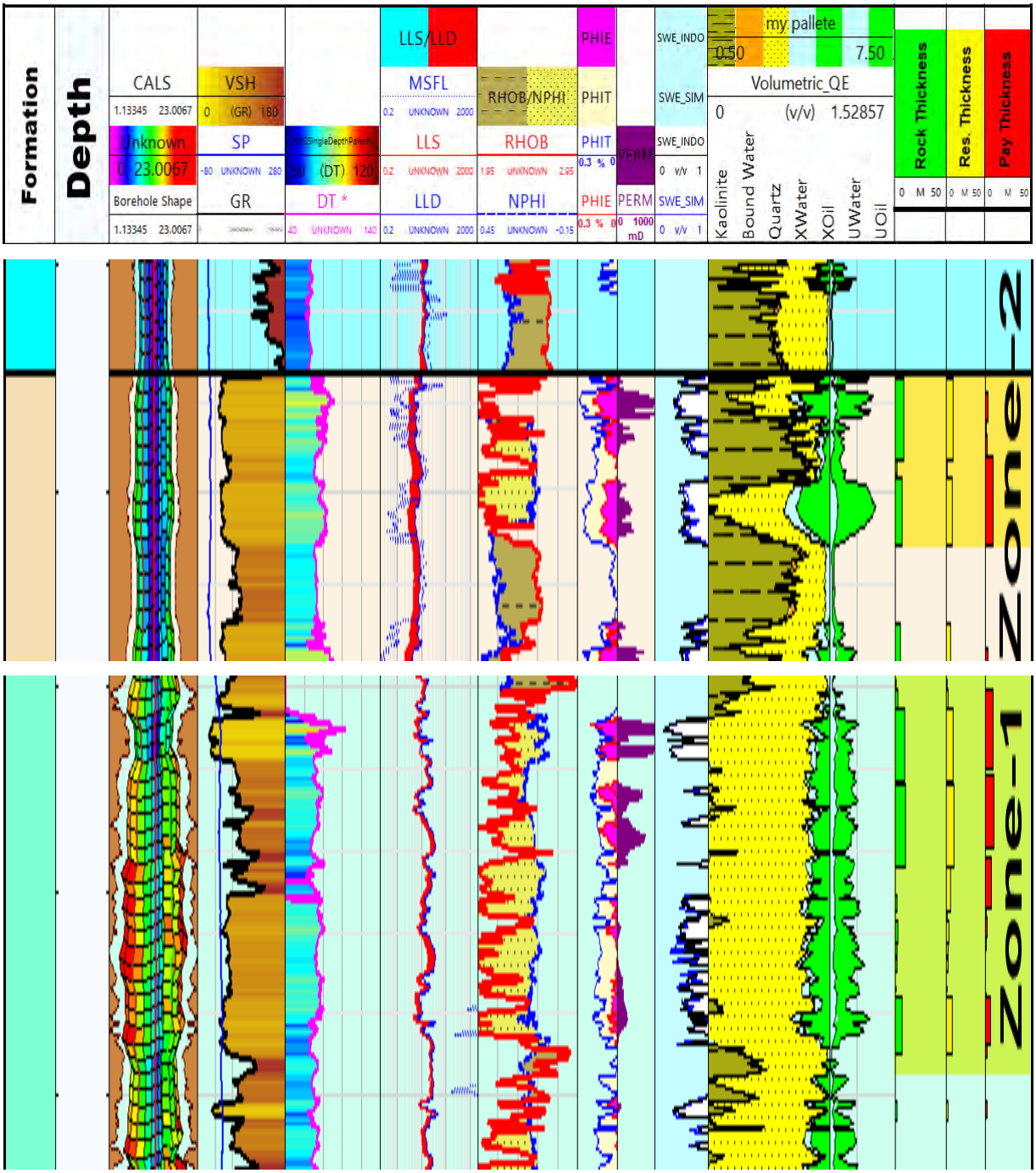

Figure 3.3a Zones of Interest in Miano-02 Well

3.6 Petro-physical results of Miano-09 well:

Like the Miano-02 well, the Miano-09 well also targets the B interval within the Lower Goru Formation, characterized by layers consisting of a mixture of shale and sand (Figure 3.4). Following are major results deducted from Petrophysical analysis of Miano-09 well. Similar to Miano-02, there is an anticipation of achieving a substantial net income from this interval, based on several key factors:

- Separation between Latro-Log Deep and Latro-Log Shallow: The distinction between the lower limit of detection (LLD) and the lower limit of quantification (LLS) suggests the presence of measurable hydrocarbons, which is economically promising.
- Low Gamma Ray (GR): A low Gamma Ray (GR) is often associated with clean, hydrocarbon-bearing sands.
- High Resistivity: High resistivity is indicative of hydrocarbon-bearing formations.
- Porosity: The presence of porosity is favorable, indicating potential reservoir capacity.
- Zone of Interest in B and C-Intervals: Similar to Miano-02, the zone of interest in the Miano-09 well extends into both the B and C-Intervals and has a thickness range spanning a few meters.
- Low Shale Volume in B-Interval Sand: In the B-Interval sand, as observed in Miano-02, the shale volume is relatively low. This suggests that a significant portion of this interval comprises potentially hydrocarbon-bearing sands.
- C-Interval Shale Baseline: In contrast, the C-Interval has a shale baseline with a shale content of 60API, indicating a higher shale content in this section of the reservoir.
- High Effective Porosity in B-Interval Sand: Similar to Miano-02, the B-Interval sand in Miano-09 exhibits high effective porosity, which is a positive sign for reservoir quality.
- Hydrocarbon Potential in B-Interval Sand: The high porosity and permeability values in the B-Interval sand suggest the potential for hydrocarbons to be present, making it a promising hydrocarbon reservoir.
- Confirmation through Log Data: The confirmation of a productive zone within the B-Interval sand is supported by the presence of NPHI (Neutron Porosity) and RHOB (Bulk Density) crossover and separation in resistivity logs. These logs provide additional evidence of the hydrocarbon-bearing potential of this zone.

Zone #1 – In correlation with Miano-02:

This Zone in the Miano-09 well, which correlates with Zone #1 in Miano-02, is identified as the highest net paying zone. It shares several similar characteristics:

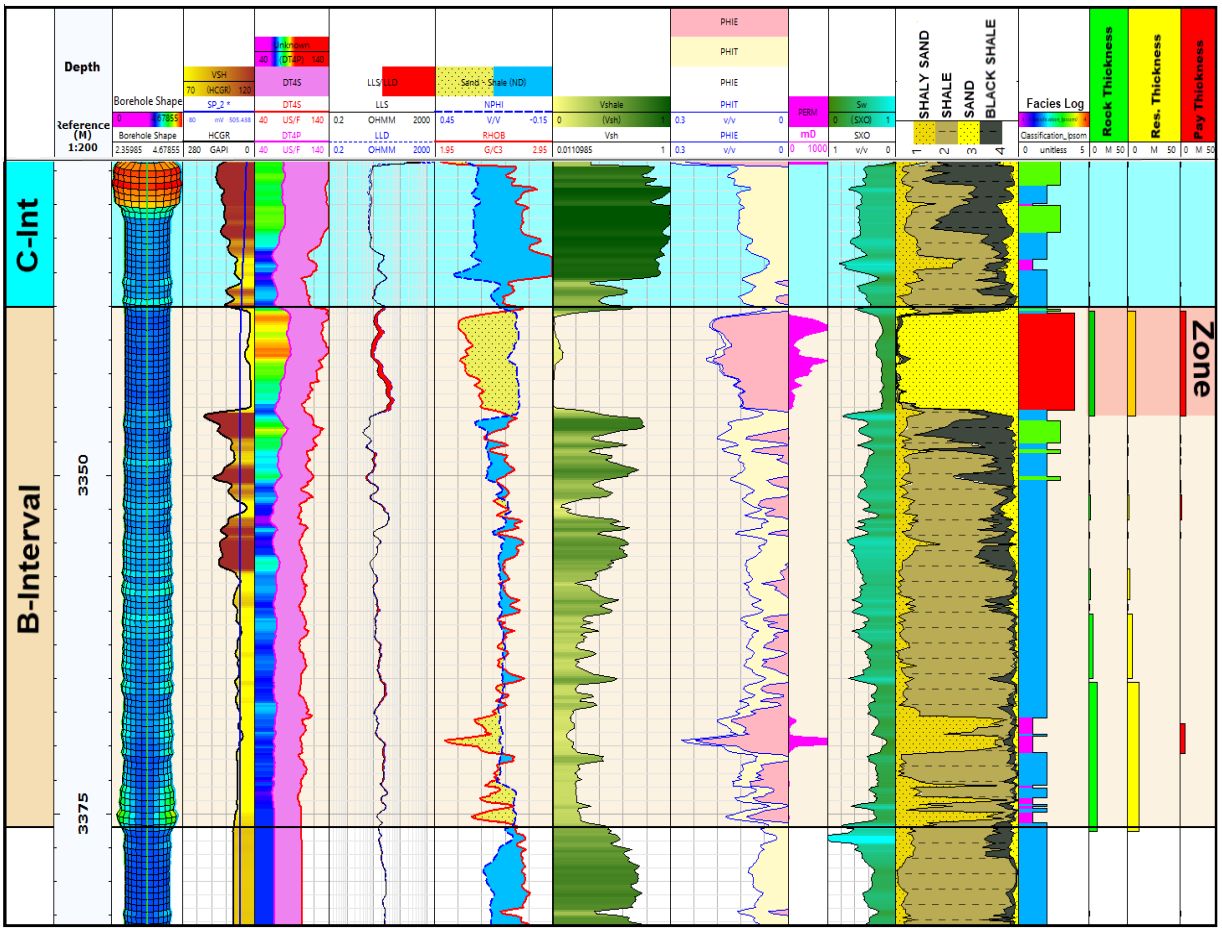

Figure 3.4: Petrophysical analysis of well Miano-09.

- High Effective Porosity and Permeability: These properties suggest good fluid retention and flow potential, making it an attractive reservoir zone.
- Low Water Saturation: Low water saturation implies a high Hydrocarbon Saturation (SHC) (SHC), indicating it as a potential gas-producing zone within the B-Interval sand.

Zone #2 - Moderate Reservoir Features: This zone in Miano-09 exhibits somewhat moderate reservoir features, similar to what was observed in Miano-02:

- High Effective Porosity and Permeability: It has high porosity and permeability, indicating good fluid retention and flow potential.
- High Water Saturation: The high water saturation suggests a lower Hydrocarbon Saturation (SHC).
- NPHI and RHOB Cross-Over: Like in Miano-02, there is a small cross-over of NPHI and RHOB, indicating a less distinct separation in resistivity logs, which may be less favorable for hydrocarbon production.

In summary, the results from the Miano-09 well mirror those of Miano-02, with a promising hydrocarbon reservoir zone in the B-Interval sand, particularly in Zone #1. This zone displays high

effective porosity, permeability, and low water saturation, making it an attractive candidate for potential hydrocarbon production. Zone #2, while still having favorable properties, exhibits somewhat lower reservoir quality compared to Zone #1. These findings are essential for reservoir evaluation and development planning in the Miano field.

3.7 Petrophysical results of Miano-10:

Miano-10, like Miano-02 and Miano-09, targets the B interval within the Lower Goru Formation, characterized by layers consisting of a mixture of shale and sand. Results are shown in Figure 3.5.

3.7.1 Interpretation:

Similar to the previous wells, there's an expectancy of achieving a substantial net income from this interval, based on several key aspects:

- Separation between Latro-Log Deep and Latro-Log Shallow: The distinction between the lower limit of detection (LLD) and the lower limit of quantification (LLS) suggests the presence of measurable hydrocarbons, which is economically promising.
- Low Gamma Ray (GR): A low Gamma Ray (GR) often indicates clean, hydrocarbon-bearing sands.
- High Resistivity: High resistivity is indicative of hydrocarbon-bearing formations.
- Porosity: The presence of porosity is favorable, indicating potential reservoir capacity.

3.7.2 Zone of Interest in B and C-Intervals:

Similar to Miano-02 and Miano-09, the zone of interest in the Miano-10 well extends into both the B and C-Intervals and has a thickness range spanning a few meters.

3.7.3 Low Shale Volume in B-Interval Sand:

In the B-Interval sand, as observed in Miano-02 and Miano-09, the shale volume is relatively low. This suggests that a significant portion of this interval comprises potentially hydrocarbon-bearing sands.

3.7.4 C-Interval Shale Baseline:

In contrast, the C-Interval has a shale baseline with a shale content of 60API, indicating a higher shale content in this section of the reservoir.

3.7.5 High Effective Porosity in B-Interval Sand:

The B-Interval sand in Miano-10 also exhibits high effective porosity, which is a positive sign for reservoir quality.

3.7.6 Hydrocarbon Potential in B-Interval Sand:

Similar to the other wells, the high porosity and permeability values in the B-Interval sand of Miano-10 suggest the potential for hydrocarbons to be present, making it a promising hydrocarbon reservoir.

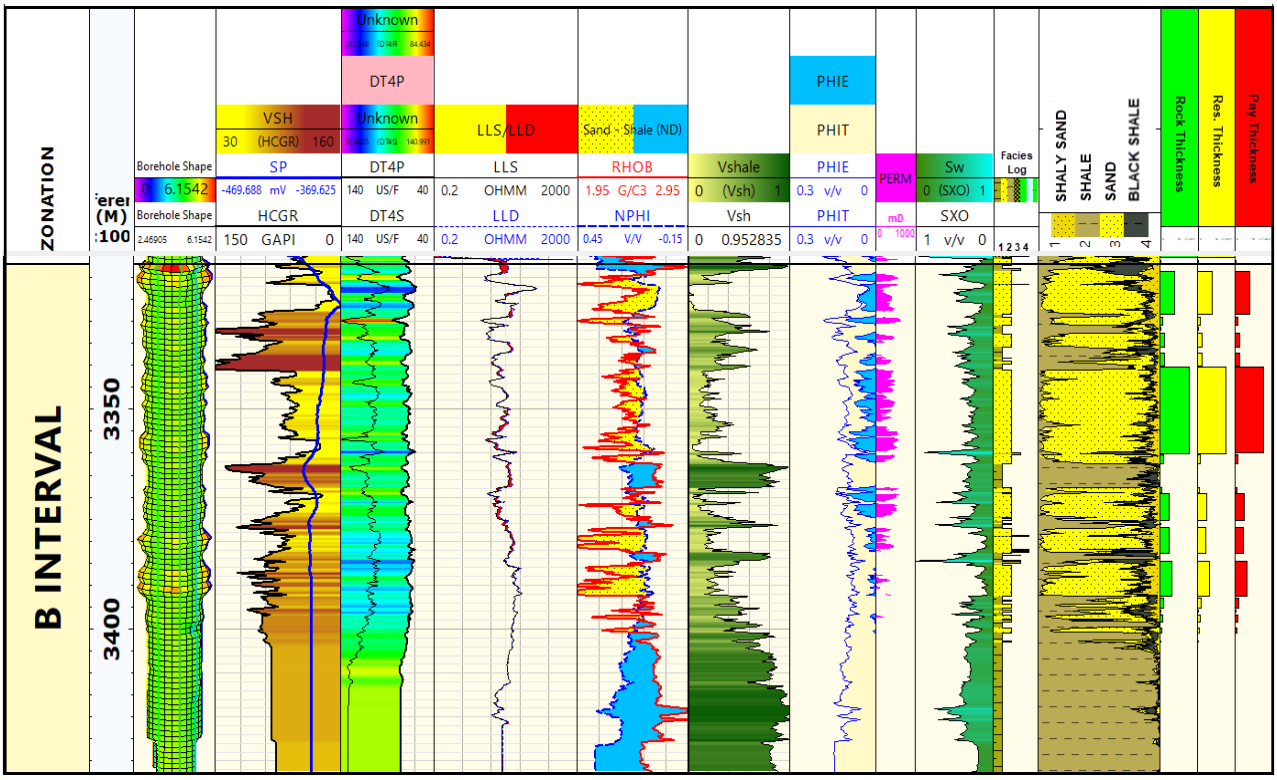

Figure 3.5: Petrophysical analysis of well Miano-10.

3.7.7 Confirmation through Log Data:

The confirmation of a productive zone within the B-Interval sand is supported by the presence of NPHI (Neutron Porosity) and RHOB (Bulk Density) crossover and separation in resistivity logs, similar to what was observed in Miano-02 and Miano-09.

Zone #1:-This zone in the Miano-10 well, which correlates with Zone #1 in Miano-02 and Miano-09, is identified as the highest net paying zone. It shares several similar characteristics:

- High Effective Porosity and Permeability: These properties suggest good fluid retention and flow potential, making it an attractive reservoir zone.
- Low Water Saturation: Low water saturation implies a high Hydrocarbon Saturation (SHC), indicating it as a potential gas-producing zone within the B-Interval sand.

Zone #2:- Zone #2 in Miano-10 exhibits somewhat moderate reservoir features, similar to what was observed in Miano-02 and Miano-09:

- High Effective Porosity and Permeability: It has high porosity and permeability, indicating good fluid retention and flow potential.
- High Water Saturation: The high-water saturation suggests a lower Hydrocarbon Saturation (SHC).

- Neutron Porosity and Bulk Density Cross-Over: Like the other wells, there is a small cross-over of NPHI and RHOB, indicating a less distinct separation in resistivity logs, which may be less favorable for hydrocarbon production.

In summary, the results from the Miano-10 well, like Miano-02 and Miano-09, indicate the presence of a promising hydrocarbon reservoir zone in the B-Interval sand, particularly in Zone #1. This zone displays high effective porosity, permeability, and low water saturation, making it an attractive candidate for potential hydrocarbon production. Zone #2, while still having favorable properties, exhibits somewhat lower reservoir quality compared to Zone #1. These findings are essential for reservoir evaluation and development planning in the Miano field. Summary of zones of interest in **Miano-2** well can be depicted in the table below.

Zones	Flag Name	Top	Bottom	Gross	Net	Net to Gross	Avg_Shale Volume	Average Porosity	Effective porosity	Avg_Water Saturation
Zone_I	ROCK	3503.13	3539.11	35.979	34.492	0.959	0.247	0.171	0.106	0.278
	RES	3503.13	3539.11	35.979	34.492	0.959	0.247	0.171	0.112	0.278
	WAT									
Zone_II	ROCK	3137.6	3171.72	34.124	23.25	0.681	0.378	0.223	0.0691	0.676
	RES	3137.6	3171.72	34.124	23.25	0.681	0.378	0.223	0.0768	0.676
	WAT									

3.8 Well Correlation:

“Well correlation" is the process of analyzing and comparing data from multiple wells to understand the spatial distribution and variations of rock layers or reservoir zones.

3.8.1. Correlation of Reservoir Zone: In the context of geological and reservoir studies, "correlation" refers to the process of analyzing and comparing data from multiple wells to understand the spatial distribution and variations of rock layers or reservoir zones. The primary focus of this correlation exercise is the reservoir zone within each of the wells. This is typically a key target for oil and gas exploration or production.

3.8.2. Spatial Variability and Thickness Changes: By performing this correlation, the objective is to gain insights into how the reservoir zone changes across the study area. This includes understanding how its thickness varies from one location to another.

3.8.3. Base Map: A "base map" serves as a reference map that provides the geographical context for the study. It usually includes important features such as well locations, geographical coordinates, and distances between key points of interest.

3.8.4. Well Positions and Distances: The base map in this case displays the positions of the individual wells being studied. This allows analysts to visualize where each well is located in relation to others. The "distance between them" mentioned likely refers to the separation between the wells, which is a crucial factor in understanding how the reservoir zone changes over space.

3.8.5. Variation in Thickness: The information provided indicates that the B-Interval of the reservoir zone exhibits a distinct trend in thickness as one moves from south to north. Specifically, as you move further north, the B-Interval becomes thicker. On the contrary, the thickness of the reservoir sand in both the B-Interval and the C-Interval remains relatively consistent. This implies that these sand layers do not show significant variations in thickness across the study area.

Well Correlation Results:

A correlation study was carried out on the reservoir zone in three wells **(**Figure 3.6), and the results of this study have offered crucial insights on the spatial variability and thickness changes within the studied area. In contrast, the thickness of the B-Interval grows as one travels northward, while the thickness of the reservoir sand remains largely unchanged across the research area. These insights are helpful for making educated decisions concerning the exploration, development, and production of reservoirs in this region. The study benefits from having a reference in the form of the base map, which shows the locations of the wells as well as the distances that separate them. The fact that the thickness of the reservoir sand is always the same provides evidence that it has a uniform composition and qualities, which is beneficial for modeling and managing reservoirs. The rise in thickness that occurs northward in the B-Interval suggests the presence of a likely geological trend or feature that may have an effect on the quality of the reservoir and the potential for hydrocarbon accumulation. In general, these findings and debates deepen our comprehension of the reservoir zone

and the variations that exist within it. As a result, they supply us with knowledge that is useful for making decisions regarding oil and gas exploration and production.

3.8.6. Northward Thickness Increase in B-Interval: The observation that the thickness of the B-Interval increases as you move northward is significant. It suggests a possible geological trend or feature in that direction, which could have implications for reservoir quality and potential oil or gas accumulation. Understanding this variation is crucial for well placement and drilling strategies, as thicker reservoir zones often indicate more favorable conditions for hydrocarbon extraction.

3.8.7. Consistent Thickness in Reservoir Sand: The stability in thickness for both the B-Interval and C-Interval reservoir sands suggests that these layers might be relatively uniform in terms of their composition and properties over the study area. This could be beneficial for reservoir modeling and management, as it implies a certain degree of predictability

In summary, the correlation study conducted on the reservoir zone in multiple wells has revealed important insights about the spatial variability and thickness changes within the study area. Notably, the B-Interval thickness increases as you move northward, while the reservoir sand thickness remains relatively constant across the study area. These findings are valuable for making informed decisions related to reservoir exploration, development, and production in this region.

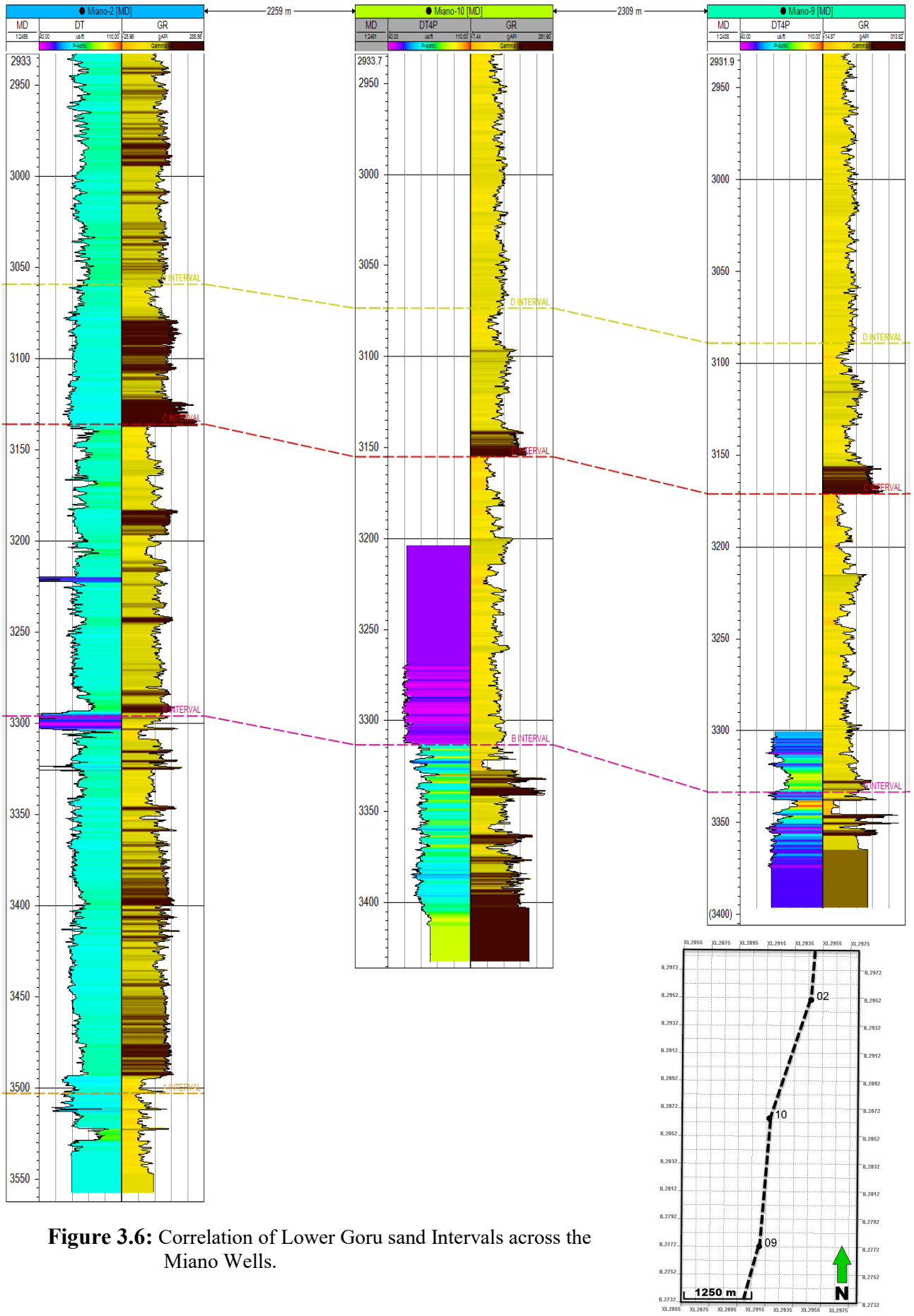

Figure 3.6: Correlation of Lower Goru sand Intervals across the Miano Wells.

CHAPTER #04

4. SEISMIC INTERPRETATION

4.1 Introduction

The primary objective of this chapter is to examine the structural interpretation of three-dimensional (3D) seismic data within the Miano Block. The process of seismic interpretation encompasses the transformation of seismic reflection data into a geological representation through the application of corrections, migration techniques, and the conversion of time to depth. The purpose of this procedure is to ascertain the coordinates and identify geologically obscured boundaries or sudden transition regions that occur as a result of the reflection of seismic waves upon reaching the Earth's surface. By amplifying the impact of heterogeneous geological conditions along the profiles, the sporadically documented travel time is transformed into dependable subsurface models. Accurate determination of the depth and geometry of the bedrock or target horizons is crucial in this context.

An integral component of exploration geophysics is seismic modeling, which entails the complex process of generating the seismic response of a given geological configuration. This might refer to either structural or stratigraphic characteristics of the geological formation being modeled. In order to accomplish this goal, geoscientists use a method called trial and error, in which they experiment with different combinations of model parameters to create a variety of seismic reactions. These model parameters include velocity distribution, physical dimensions, and structural complexities. The end goal is to establish a model that demonstrates a good connection with observed seismic sections and, as a result, represents a credible picture of the genuine underlying lithology. This will be accomplished by finding a model that fits these criteria.

The once difficult process of learning via trial and error has become easier to manage as a result of the introduction of sophisticated electronic computers that are equipped with interactive interfaces. In order to improve the effectiveness and precision of seismic modeling, geoscientists now have the ability to rapidly modify processing settings and witness immediate results on their screens. The employment of geological modeling and automated reflection picking has become more frequent in modern interpretation processes. These two techniques contribute an additional level of precision to the process.

Furthermore, advancements in theoretical knowledge have led to exciting applications in hydrocarbon detection. By analyzing the reflection waveforms, geoscientists can directly identify potential hydrocarbon reservoirs. This is achieved by detecting areas with substantial impedance-

contrast across interfaces, leading to robust reflections known as "bright spot" features. These bright spots often signal the presence of gas-sand formations, where notable impedance contrast exists between the reservoir and surrounding media, yielding prominent reflection signals.

In modern seismic modeling, one of the primary focuses is on bright spot interpretation. This technique involves computing seismic responses for diverse geologic models and comparing them to the observed seismic section. The model whose synthetic seismic response closely matches the actual seismic data is considered the most accurate representation of the subsurface. However, it is crucial to emphasize that when generating the time stack section for bright spot interpretation, amplitude-distorting processes should be avoided, ensuring fidelity in the seismic data analysis. By adhering to these best practices, geoscientists can unravel the hidden mysteries of the subsurface and gain valuable insights into potential hydrocarbon reservoirs and geological structures (Al-Sadi, 1980).

4.2 Synthetic Seismic Modeling & well correlation

Seismic synthetic modeling is a method used to predict subsurface seismic responses by generating synthetic seismograms through the convolution of reflection coefficients and seismic wavelets. These seismograms help identify geological horizons on seismic data by comparing well log lithology with seismic reflections. The accuracy of the link between synthetic seismograms and seismic data depends on a number of things, such as how accurate well log data is, how well seismic data processing techniques work, and how well wavelets can be extracted. The process for generating synthetic seismograms involves loading a well's LAS files, creating a 1D forward modeling project, converting sonic log to two-way travel time, calculating P and S wave velocities, constructing a time-depth chart using velocity logs, computing acoustic impedance using velocity and density logs, derived reflection coefficients from time-scaled velocity log, and generating a first-order Ricker wavelet with specific parameters.

Correlating synthetic seismograms with seismic data reveals minor mismatches, but the well's DT log aids in confirmation of horizons. Accurate seismic data interpretation requires integrating seismic and well data, with prominent reflectors correlated with well tops to identify six horizons. The area's depositional pattern influences line trends and fault visibility.

The study focuses on the evolution of seismic interpretation in the Miano area, which has evolved from simple structural trap detection to a comprehensive analysis of multiple parameters. This iterative process involves incorporating well data, generating synthetic seismograms, and careful tie-ins to enhance the accuracy of subsurface modeling and prospect assessment. Synthetic seismograms are one-dimensional representations of acoustic impedance energy propagating through earth's

layers, created by convolving reflection coefficients from digitized sonic and density logs with seismic wavelets. The synthetic seismograms to correlate Miano-02 well log lithology with seismic reflections is presented in Figure 4.1. The quality of tie between synthetic seismogram and seismic data is satisfactory however it depends on factors such as well log quality, seismic data processing, and wavelet extraction capability.

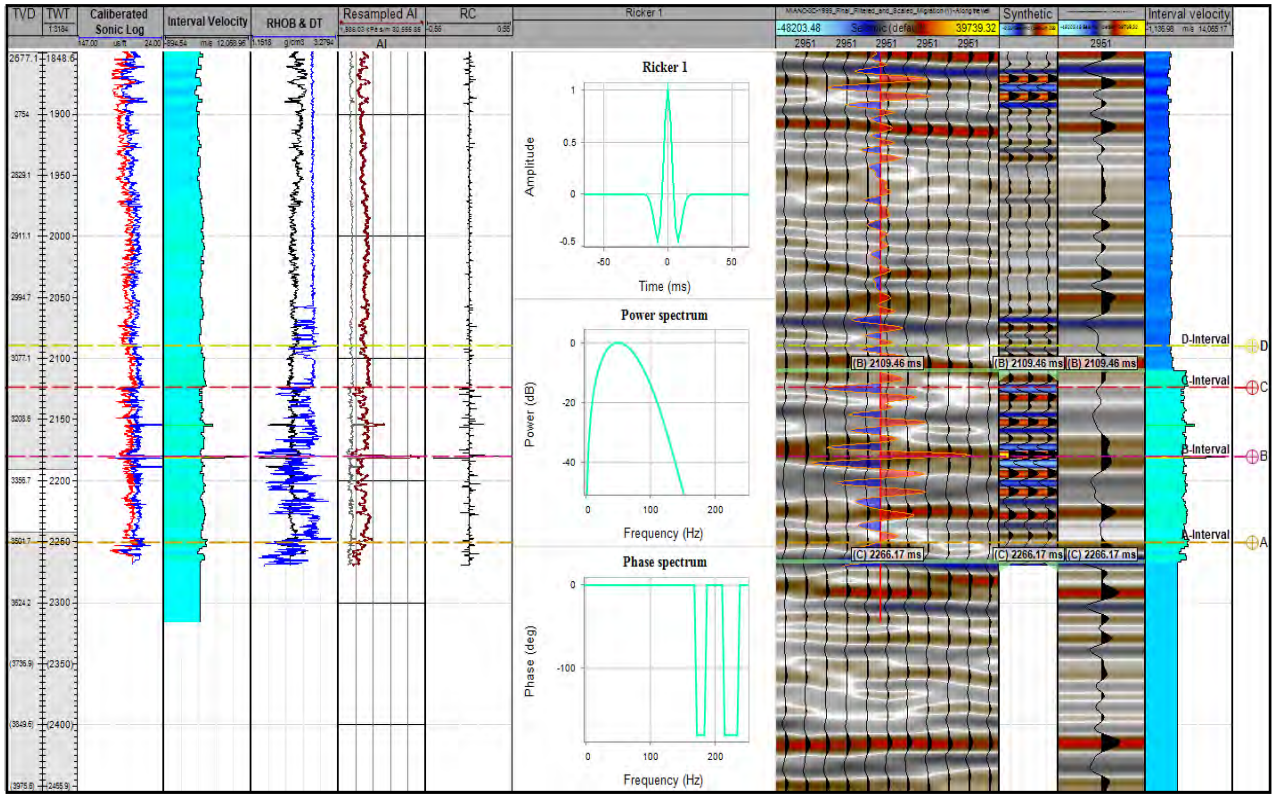

Figure 4.1: Synthetic seismogram of Well Miano-02

Correlated synthetic seismograms with seismic data revealed minor mismatches, but the correlation helps confirm horizon interpretations. Accurate seismic data interpretation requires integrating seismic and well data, with prominent reflectors correlated with well tops to identify the horizons.

4.3 Marking and identification of seismic horizons:

It is important to be able to tell the difference between the different horizons on seismic sections if you want to correctly interpret seismic data. This is true whether the interpretation is based on how the data is put together or how it is put together. To reach this goal, the seismic data is compared with the data from the well tops and with what was already known about the area's geology. The first step in figuring out what seismic data means is to find and outline important reflectors, also called horizons, on seismic sections. Horizons is what most people call these types of geological features. A reflector, which is also called a horizon, is more specifically a line or line of demarcation between two different rock formations.

After using the same methods to mark six important stratigraphic horizons on the seismic profiles, all of the sections were then connected at the tie points that went with them. The chosen reflectors are strong and have a pattern that can be followed along the seismic profile. Because of how well they work, these reflectors were chosen. On top of that, it has been shown that these seismic reflectors are linked to tie points that have been seen in other seismic lines in the area. The difference in acoustic impedance that comes from the different types of rock makes it much easier to find these reflectors. As a geoscientist, I was able to find horizons even though I didn't have VSP data. I did this by using the depths of formations from the well top data of Miano-7 and other wells in the Miano area. All of these wells were in the Miano area. Also, the depths were worked out by using the interval and average velocities that were found when the seismic data was processed.

4.4 Results

Results are discussed as per figures presented and description of each Figure is given prior to it.

4.4.1 Seismic Section Interpretation Results

The seismic section presented in Figure 4.2 corresponds to seismic interpretation, which is a vital step of any deep subsurface analysis.

- The seismic section is oriented North South and spans a lateral distance of approximately 3Km and a vertical range of 2.9 seconds.
- It captures the structural features and geological stratigraphy present within this block of interest.

- **Key Horizons:**
  - Within the seismic section, several key horizons have been identified and marked for interpretation purposes.
  - Notable horizons include A-interval, B-interval, C-interval, and D-interval of Lower Goru formation which contain economic sand reservoirs and stratigraphic units.
- **Stratigraphy:**
  - The interpretation of the seismic section reveals a well-defined stratigraphy characterized by distinct and continuous reflectors.
  - These reflectors allow us to correlate geological units and formations across the section.
  - The seismic data provides valuable insights into the geological history and sedimentary sequences present in the subsurface.
- **Structural Features:**
  - Structural features such as faults and stratigraphy are marked on the seismic section.

- There were no notable structural faults observed however several minor faults were not taken into account since they do not interfere with reservoir geometry.
- Fluid migration and reservoir compartmentalization was done based on this interpretation.

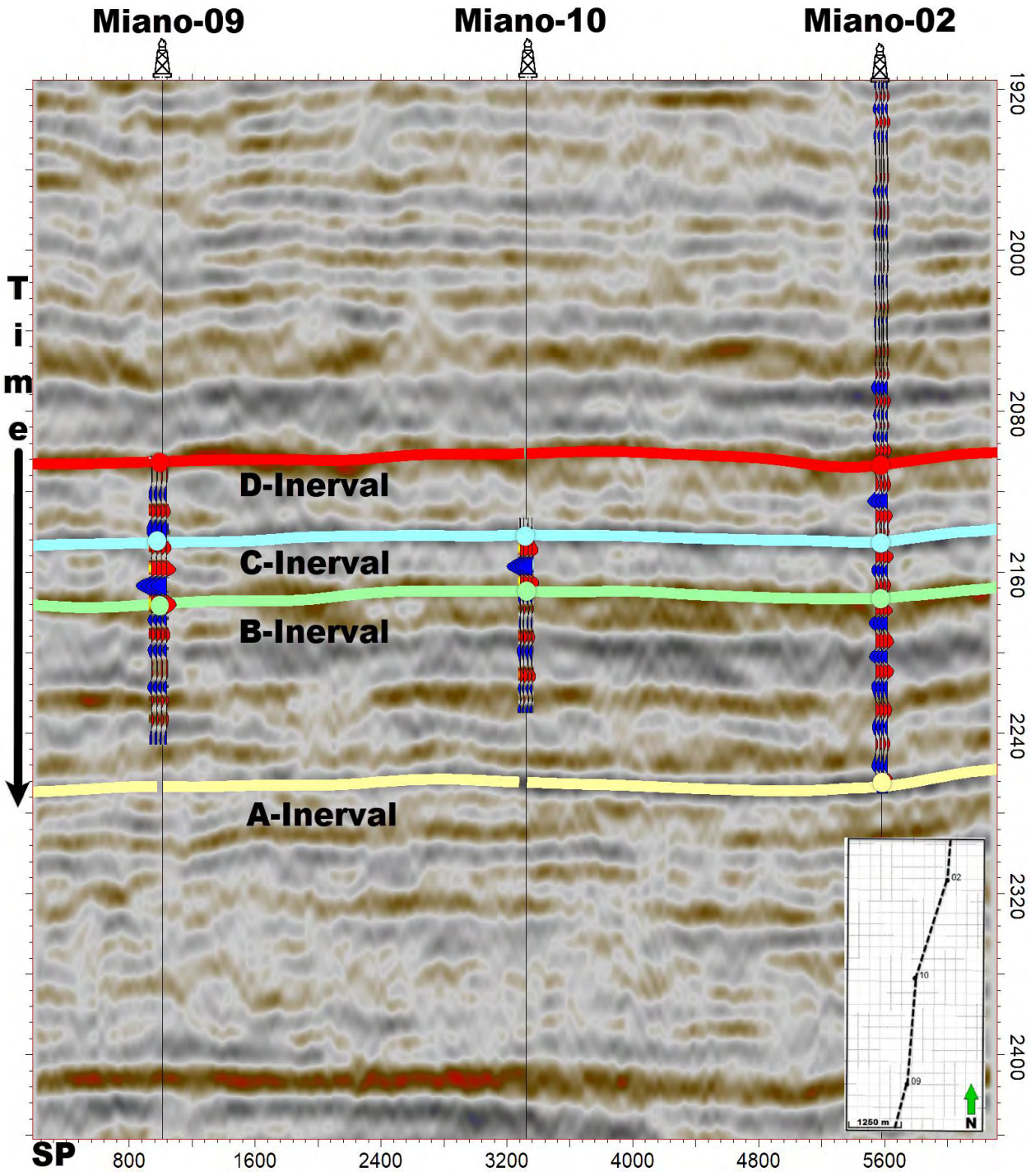

Figure 4.2: Interpreted seismic section showing a composite line across all the wells through seismic cube.

- **Amplitude Analysis:**
  - Amplitude analysis reveals variations in seismic response, including bright spots, dim zones, and amplitude anomalies.
  - Such amplitude anomalies are indicative of potential hydrocarbon accumulations and reservoirs, B-Interval contained a zone with such anomaly.
  - These anomalies warrant further investigation as potential drilling targets.
- **Reservoir Identification:**
  - The seismic section aids in the identification of potential reservoirs or pay zones.
  - Noteworthy areas within the B-Interval show favorable characteristics, such as high amplitude, continuity, and thickness, have been identified as potential hydrocarbon reservoirs.
- **Geological Insights:**
  - The seismic data provides valuable geological insights into the subsurface environment.
  - Interpretation of seismic facies, seismic geomorphology, and reflections assists in understanding the depositional environments, lithological variations, and geological history.
- **Uncertainty and Limitations:**
  - It is important to acknowledge the uncertainties associated with the seismic interpretation, including data quality limitations and assumptions made during processing and modeling.
  - Careful consideration of these uncertainties is essential for a robust interpretation.
- **Conclusion:**

  In conclusion, the interpretation of this seismic section has provided valuable information about the producing layer's horizontal variation, structural features associated with it, and potential zones within the block for further analysis. These zones will guide further exploration and appraisal activities in this region.
- **Recommendations:**

  Based on the seismic section interpretation, we recommend focusing on specific areas of interest for further investigation, including detailed reservoir characterization studies and potential drilling opportunities.

4.4.2 Results and Discussion: Time Contour Maps of A, B, C, and D-Intervals

This section delves into the intricate details revealed by the time contour maps of intervals A, B, C, and D within the Lower Goru Formation Figure 4.3. These maps are pivotal in unraveling the subsurface geological framework in time domain and structural attributes of the study area.

- Temporal Distribution and Sedimentation Patterns: The time contour maps offer a compelling visualization of the temporal distribution of seismic horizons. One prominent observation is the consistent expansion of horizons in a west-to-east direction. This spatial pattern strongly suggests a historical trend of sedimentation from west to east across our study region. Such insights into sedimentation patterns provide critical context for understanding the geological evolution of the area.
- Interval-Specific Two-Way Travel Time (TWT): For each of the four intervals studied, distinct two-way travel time (TWT) ranges have been delineated on the time contour maps:

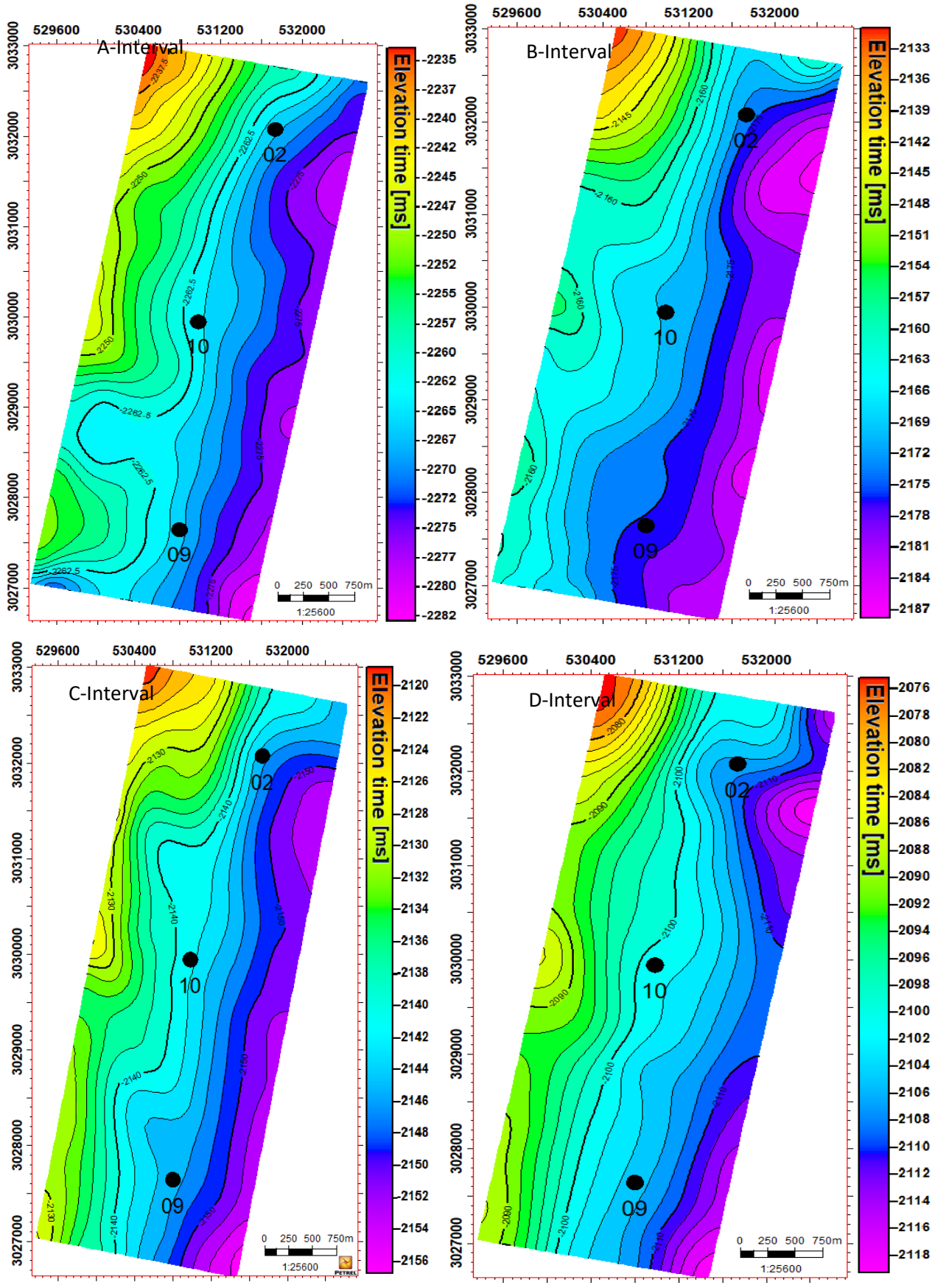

Figure 4.3: Two way time contour maps of A, B, C, and D-Intervals respectively as mention above in each Figure.

- D-Interval: This interval exhibits a TWT range spanning from 2076 to 2118 microseconds. These values are fundamental for accurately assessing depth-related properties.
- C-Interval: The C-Interval encompasses a TWT range of 2120 to 2156 microseconds, contributing to our depth conversion calculations.
- B-Interval: Within the B-Interval, the TWT range extends from 2133 to 2187 microseconds. This interval holds paramount significance for understanding subsurface structures.
- A-Interval (Sember Formation summit): The A-Interval, represented by the Sember Formation summit, is characterized by a TWT range of 2235 to 2282 microseconds. Its unique timing provides important insights into its stratigraphic position.
- Fault Features and Anomalies: While the time contour maps do not reveal significant anomalies, they do illuminate the presence of step faults and fault splays within the study section. These fault features, although not conspicuous anomalies, hold significance for reservoir compartmentalization and fluid migration pathways. Further investigations into their characteristics are warranted.
- Visualization and Three-Dimensional Representation: Beyond static images, the temporal contour maps provide a dynamic visual representation of the subsurface. Figure 4.4, a three-dimensional representation of the highlighted horizons, adds another dimension to our understanding. It vividly illustrates the direction and dip of these critical horizons, aiding in structural interpretations.
- Interpretation Insights: The analysis of the temporal contour maps uncovers nuanced subsurface characteristics. Notably, the maps reveal that the sand formations exhibit a relatively uniform elevation in the north-eastern region with minimal elevation fluctuations. Conversely, the western portion displays greater depth, indicating a discernible slope from east to west. These observations serve as key indicators of subsurface structural trends and sedimentary patterns within the study block.
- Conclusion and Geological Inference: Contour maps helped us understand the Lower Goru Formation's structural characteristics and fault distribution. These maps are crucial for comprehending the research area's subsurface geology.

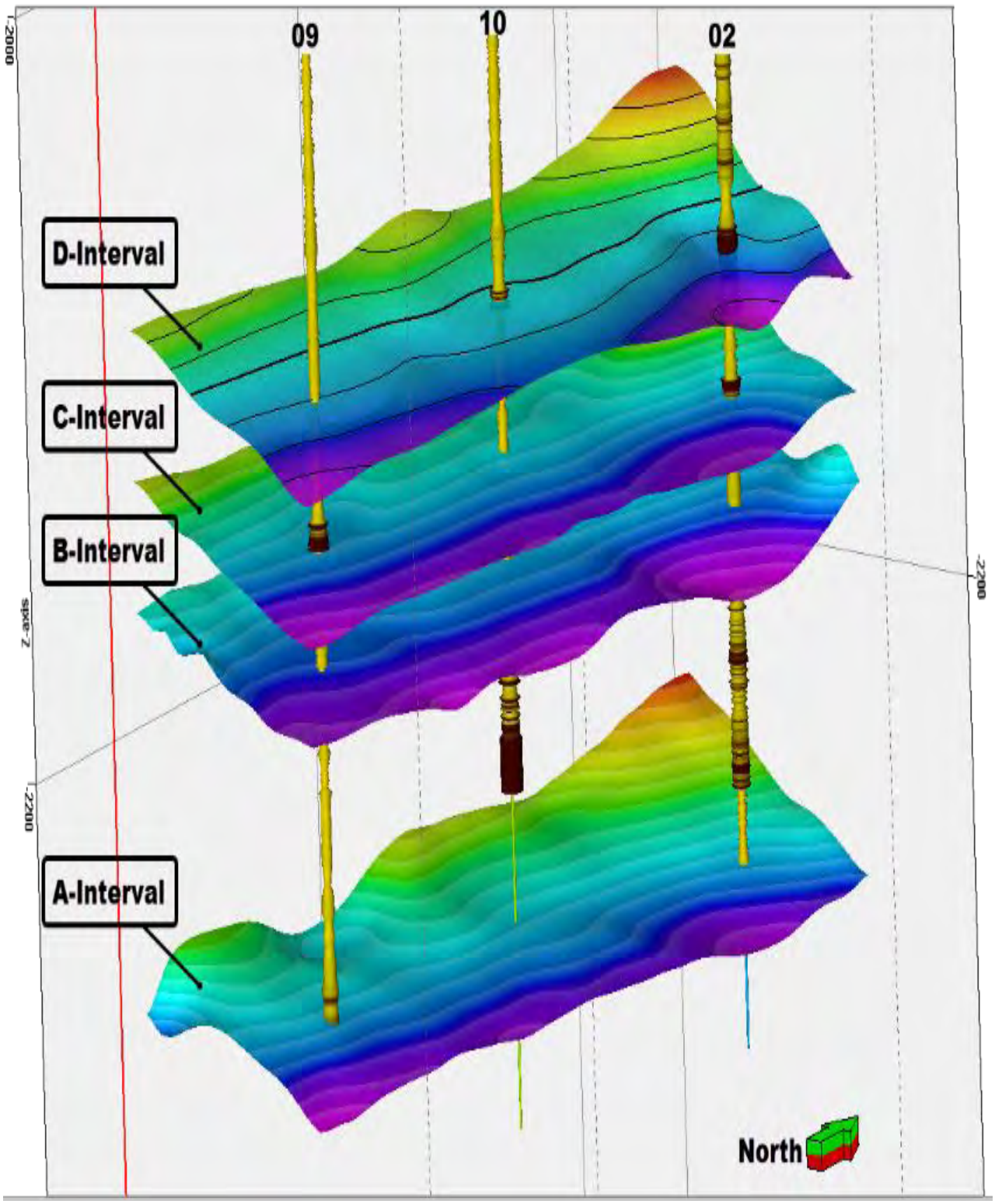

Figure 4.4: 3D view and orientation of top surfaces of sand Intervals of Lower Goru formation.

CHAPTER #05

5. ROCK-PHYSICS MODELLING

5.1 Introduction:

Rock physics modelling, an interdisciplinary approach, combines geology, Petrophysics, physics, and mathematics to enhance decision-making in characterization of the rocks potentially viable for energy resources and continues to evolve with advancements in technology. It not only improves reservoir characterization but also hydrocarbon exploration and Geotechnical investigations, which are concerned with elastic properties that are affected by mineral composition. The importance of elastic properties, Petrophysical properties, fluid effects, mineralogy, porosity, pore geometry, rock texture, anisotropy, laboratory measurements, forward and inverse modelling, seismic inversion, hydrocarbon exploration, and reservoir characterization cannot be overstated. The elastic properties of rocks, including Young's modulus, Poisson's ratio, and bulk modulus, control how they react to stress and strain. The transmission and reflection of seismic waves in rocks are greatly influenced by Petrophysical parameters, including porosity, permeability, and mineralogy. The seismic properties are influenced by fluid effects, which encompass the characteristics and concentration of fluids present within rocks. The determination of elastic properties is significantly influenced by the mineral composition, as different minerals exhibit distinct characteristics such as densities, elastic moduli, and pore spaces. Porosity and pore geometry are fundamental to rock physics modeling, with high porosity and well-connected pores resulting in reduced seismic velocities and increased reflectivity. Rock texture and anisotropy describe the arrangement of minerals and fractures within rocks, with anisotropic rocks having different seismic properties in different directions.

Rock physics modelling is also helpful in obtaining confidence in the quality of Petrophysical curves and discriminating between reservoir rocks and non-reservoir rocks based on elastic characteristics cross plots. Both of these benefits can be attained through the use of cross plots. There is also discussion on the various methods for estimating Petrophysical input, such as shale volume, porosity, and water saturation.

Following the modelling of well logs, uncertainty analysis is carried out using the Monte Carlo simulation. These simulations have been designed with the purpose of determining whether or not the rock physics model accurately reproduces the variability in the log data. These probabilistic models, which symbolize the distribution of the shale, are constructed, and then simulations may be run using them.

Rock physics modeling is an interdisciplinary field that combines geology, Petrophysics, physics, and mathematics to better understand subsurface formations and improve decision-making in the oil and gas industry and other geophysical applications. The following are the most important aspects of rock physics modelling:

- **Elastic characteristics:** The elastic properties of rocks determine their response to stress and strain. These include Young's modulus, Poisson's ratio, and bulk modulus. Rock physics models aim to correlate elastic properties with porosity, mineral composition, and fluid content.
- **Petrophysical Properties:** Rock physics models frequently include porosity, permeability, and mineralogy. These characteristics can have an impact on how rocks transmit and reflect seismic waves.
- **Fluid Effects:** The seismic properties of rocks are determined by their water, oil, or gas content and saturation. Models of rock physics explore how fluid content impacts earthquake reactions.
- **Mineralogy:** The mineral composition influences rock flexibility. The transmission of seismic waves by rocks is influenced by mineral densities, elastic moduli, and pore spaces.
- **Porosity and Pore Geometry:** The modelling of rock mechanics is dependent on pore space distribution and shape. Porosity and interconnected pores lower seismic velocities while increasing reflectance.
- **Forward and Inverse Modelling:** Rock physics models allow for inverse and forward modelling. Based on rock parameters, forward modelling predicts seismic wave behavior in a rock or reservoir. Inverse modelling, on the other hand, predicts rock attributes using seismic data.
- **Seismic Inversion:** Seismic inversion employs rock physics modelling. The underlying rock porosity, fluid content, and lithology are determined by inverting seismic data.

Applications of rock physics modelling involve geomechanical investigations and reservoir elastic properties calculation to understand fluid behavior and to estimate the reserves. Data on shear waves is essential for determining elastic parameters such as the V_P vs V_S ratio, Poisson's Ratio, and Elastic Impedance, all of which contribute to the classification of fluids and the characterization of reservoir rocks. Shear wave prediction, on the other hand, is not without its difficulties. These difficulties include a lack of shear wave data in the vast majority of wells, a lack of contrast in elastic properties between the various lithofacies, and the requirement to understand how elastic characteristics change with variations in pressure and temperature.

The empirical regression methods and the effective medium theory are the two primary classifications that are utilized in shear wave prediction. There is no one method that can be used everywhere; therefore, it is required to calibrate the data locally. Quick look methods, such as multi-linear regression and neural network techniques, deliver quick and acceptable findings without making any assumptions about pore geometry or rock moduli. These methods are also known as "quick look" methods. When it comes to predicting shear wave, these approaches make use of input data such as GR, resistivity, neutron, density, and depth.

When attempting to estimate the final shear wave, it is helpful to compare the measured logs to the modelled logs. It is possible to apply multi-linear regression models to wells with missing or erroneous shear wave curves if the models were constructed using well logs that had data of a high quality. On the other hand, people may have a tendency to like the curve that has the highest correlation.

5.2 The construction of Rock physics Model

It is critical to develop an efficient rock physics model (RPM) for reservoir behavior prediction. This research pertains to build the elastic rock physics modelling of Lower Goru sand shale intervals in middle Indus Basin along with the uncertainty analysis using Monte Carlo simulation. A workflow is proposed using an effective modelling for different sand-shale rock composition taking in account the matrix, fluids, and pores etc. The primary objective of this modelling technique is to predict and remodel the effective attributes such as density and velocities after incorporating effective minerals. This is quite useful in a variety of exploration and production settings to recognize the behavior of reservoir rock. Workflow followed for RPM is given in Figure 5.1.

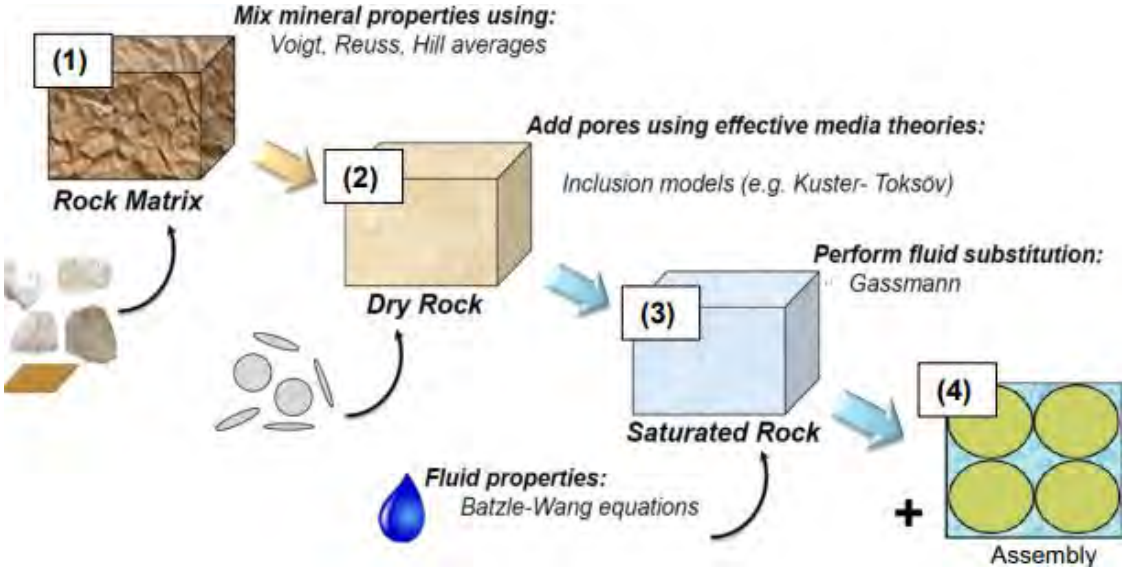

Figure 5.1: Workflow for construction of a rock physics model.

5.2.1 Voigt–Reuss–Hill (V–R–H) average

In order to develop a model, first step is to determine the mineral properties. To build an effective mineralogy, it is better to apply boundaries and averages to account for the fact that the grain arrangement is uncertain. In quest of estimating the effective moduli of minerals, simplistic approach to calculate the average of V-R bounds, referred to as V-R-H average.

$$M_{VRH} = \frac{M_V + M_R}{2} \tag{5.1}$$

5.2.2 Self-consistent approximation (SCA) model

The SCA model was proposal of Budiansky and Hill, (1965). This model takes into account the pore geometry and interaction of inclusions adjacent to each other so it can be used for rocks with slightly larger inclusion concentrations. Berryman, (1995) defines the SCA for N-phase composites in a general manner given in equation 5.4 and 5.5. This technique is used to incorporate complex components and fluid-filled pores with variable geometries into the elastic characteristics of rocks.

$$\sum_{i=0}^{n} x_i (K_i - K'_{sc}) \beta'^i \tag{5.2}$$

$$\sum_{i=0}^{n} x_i (\mu_i - \mu'_{sc}) \zeta'^i \tag{5.3}$$

Here, i denotes the ith material, xi, is volume fraction Ki and μi equals bulk & shear moduli. $\beta' i$ and $\zeta' i$ are geometric factors of inclusions. $\beta' i$ and $\zeta' i$ can be defined in terms of Km and μm i.e bulk and shear modulus of matrix.

$$\beta'^i = \frac{K_m + \frac{3}{4}\mu_i}{K_i + \frac{3}{4}\mu_i + \pi\alpha\mu_m \frac{3K_m + \mu_m}{3K_m + 4\mu_m}} \tag{5.4}$$

$$\zeta'^i = \frac{1}{5}\left[\frac{8\mu_m}{4\mu_i + \pi\alpha\mu_m\left(1+2\frac{3K_m + \mu_m}{3K_m + 4\mu_m}\right)} + \frac{K_i + \frac{2}{3}(\mu_i + \mu_m)}{K_i + \frac{3}{4}\mu_i + \pi\alpha\mu_m \frac{3K_m + \mu_m}{3K_m + 4\mu_m}}\right] \tag{5.5}$$

5.2.3 Kuster–Toksöz (K–T) model

K-T model calculates the dry rock properties of rock. It assumes the pore shape to be ellipsoidal, which is defined by aspect ratio. There is a decrease in velocity with an increase in the porosity of an object (Toksöz et al, 1976). Keys and Xu (2002) used a simplistic approach to estimate effective modulus of dry rock by making an assumption of dry-rock Poisson's ratio is constant with respect to porosity.

$$K_{dry} = K_m (1 - \phi)^p \tag{5.6}$$

$$G_{dry} = G_m (1 - \phi)^q \tag{5.7}$$

Here, Kd and μd represents bulk & shear moduli of dry rock, having porosity φ. Km and μm are the effective bulk & shear moduli of mineral building a rock respectively.

K-T approach is also used to determine the elastic characteristics of fluid mixture (oil, gas, water), assuming that the fluid is present in the pores. Stiffness can be found using relation:

$$\frac{K_{Ke}}{K_k} = \frac{1+\left[4\mu k\left(K_f-K_k\right)/\left(3K_f+4\mu_k\right)K_k\right]S}{1-\left[3\mu k\left(K_f-K_k\right)/\left(3K_f+4\mu_k\right)K_k\right]S} \tag{5.8}$$

$$\frac{\mu_{Ke}}{\mu_k} = \frac{(1-S)\left(9K_f+8\,\mu_k\right)}{9K_k+8\,\mu_k+S\,(6K_k+12\,\mu_k)} \tag{5.9}$$

Where, φ_f, φ_k, are fluid volume; K_k, μ_k are bulk & shear modulii. K_{ke} and μ_{ke} are effective bulk & shear moduli of fluid.

5.2.3 Gassmann's equation

Gassmann (1951) determines the modulus of rock saturated with respect to known moduli of dry rock, minerals, and pore fluids. Gassmann's equations are applicable only in the absence of stiffness in the pore filling fluid. The saturated moduli of rock are expressed as:

$$K_{sat} = K_{dry} + \frac{(1-\frac{K_{dry}}{K_m})^2}{\frac{\varphi}{K_f}+\frac{(1-\varphi)}{K_m}-\frac{K_{dry}}{K_m{}^2}} \tag{5.10}$$

$$\mu_{sat} = \mu_{dry} \tag{5.11}$$

Bulk modulus of porous rock frame (K_{dry}) is given by:

$$K_{dry} = \frac{K_{sat}\left(\frac{\phi K_{matrix}}{K_{fluid}}+1-\phi\right)-K_{matrix}}{\frac{\phi K_{matrix}}{K_{fluid}}+\frac{K_{sat}}{K_{matrix}}-1-\phi} \tag{4.12}$$

Here K, K_d, K_m and K_f represents the bulk modulus of rock saturated, dry rock, mineral, and pore fluid, respectively. μ and μ_d refers to shear modulus of saturated and dry rock. φ is the porosity.

5.2.4 Batzle and Wang relation.

To obtain the elastic properties of saturated rock, Gassmann relation is used by adding the pore fluids to the dry rock. Then we determine the velocities of the P and S-waves. The flow chart of constructed rock physics model is given as:

After modeling of well logs, the uncertainty analysis was done using Monte Carlo simulation. The main objective of these simulations is to ensure that the rock physics model reproduces the log data variability. Although rock physics models provide deterministic correlations between input and output parameters such as Vp, Monte Carlo analysis assigns uncertainties to each variable and predict the output respectively. As a result, probabilistic models are generated signifying the mineral distribution. These simulations can also be used to predict the production effects on elastic attribute. The construction of Rock physics Model

It is critical to develop an efficient rock physics model for reservoir rock characterization. This research emphasizes on the elastic rock physics modelling of Lower Goru sands in Middle Indus basin along with the uncertainty analysis using Monte Carlo simulation. A workflow is proposed using an effective modelling for different rock compositions taking in account the matrix, minerals, fluids, pores etc. The primary objective of this modelling technique is to predict and remodel the effective attributes such as density, velocities, and moduli after incorporating significant minerals. This is quite useful in a variety of exploration and production settings to recognize the behavior of reservoir rock. Workflow followed for RPM is given in Figure 5.1.

Firstly, we select the formation minerals and their respective general properties trend. Lower Goru contained clay, sand and shale minerals. Elemental log analysis shows that significant minerals in shale are clay, quartz and shaly content. We propose an approach of calculating the equivalent elastic modulus of rock matrix using the SCA model.

Secondly, we analyze the pore and fluid properties. Shale is a dense, low-permeable mostly containing water. The clay mineral can absorb more fluids due to its huge micro-pore volume and surface area (Ding et al. 2012). Sands mostly contain quartz with high to medium porosity i.e. why it has a lot of bound water and adsorbed gas. This research divides pores into two types: disconnected micro-pores containing immovable fluid and connected micro-pores containing moveable fluid (Zhang et al. 2015a, b). The K-T model assumes that immobile fluid micro-pores are sparsely distributed in shale with limited connection. And the movable fluid micro-pores are connected. So the dry pores are added using K-T and PEM models, then saturated with Gassmann low-frequency relations. In this approach. The effective Rock physics modelling workflow can be summarized as follows:

- Calculation of matrix properties i.e. clay, sand and shale.
- Using V–R–H average, the elastic modulus parameters of minerals (clay, koalinite and quartz) are estimated.
- To estimate dry rock elastic properties, pores and cracks are added using K-T model. The fluid properties i.e. bulk modulus of brine is estimated using Batzle and Wang relation.
- To obtain the elastic properties of saturated rock, Gassmann relation is used by adding the pore fluids to the dry rock.
- Then we determined the density and velocities of the P and S-waves based on these models and compare it with recorded well logs data.

5.3 Modelling Results:

The rock physics modeling conducted on the Lower Goru Formation within the Miano Gas Field played a crucial role in purifying log responses and validating predicted S-wave logs. This research aimed to gain deeper insights into the factors influencing the behavior of seismic waves. When comparing the results of the modeled P-wave velocity (VP), S-wave velocity (VS), and density logs with real-world well-log data from the Lower Goru Formation, several observations emerged.

5.3.1. Consistent Sample Distribution Pattern: One noteworthy finding was the consistent sample distribution pattern demonstrated by the rock physics models. This pattern closely mirrored the geological parameters observed in the Lower Goru Formation. The alignment between the models and geological reality strengthens the credibility of these rock physics models as reliable forecasting tools within this specific geological setting.

5.3.2. Robust Correlations in Cross plots: The results of cross plot research revealed exceptionally robust correlations, underscoring the intricate relationships between rock properties and seismic reactivity. These correlations provide valuable insights into the way different rock parameters interact and influence seismic responses, contributing to a deeper understanding of the subsurface.

5.3.3. VP Values and Porosity-Fluid Content Relationship: One key observation was the significant convergence of VP values in the models with the actual log data, as demonstrated in error cross plots. This convergence was particularly evident in areas with increased porosity and fluid content, where VP values consistently trended downward. While occasional discrepancies were noted, where the model understated VP, these discrepancies indicated the presence of complex underlying heterogeneity and anisotropy that were not fully captured by the model's simplifications. This highlights the importance of considering the geological complexity of the formation in seismic modeling.

5.3.4. Parallel Patterns in VS Values: VS values were found to follow parallel patterns with very minor variances associated with the mechanical properties of the rocks. This consistency suggests that the mechanical behavior of the rocks within the Lower Goru Formation has a relatively uniform influence on S-wave velocity, as modeled.

5.3.5. Density Logs and Lithology Agreement: Density logs exhibited remarkable agreement with the modeling results, confirming the strong relationship between lithology and density within the Lower Goru sands. This alignment underscores the accuracy of the models in predicting density based on rock composition.

In summary, the validation process demonstrated that the rock physics models successfully predict seismic properties within the specific geological environment of the Lower Goru Formation in the Miano Gas Field. The convergence of VP values in areas with increased porosity and fluid content,

as well as the consistent patterns in VS values and density logs, further support the reliability of these models. This rigorous validation enhances the applicability of these rock physics models, making them valuable tools for enhancing the understanding of subsurface reservoir features in the Lower Goru Formation. These models can play a pivotal role in subsequent analyses, such as Geostatistical inversion, within the Miano Gas Field, aiding in more informed decision-making in exploration and production activities.

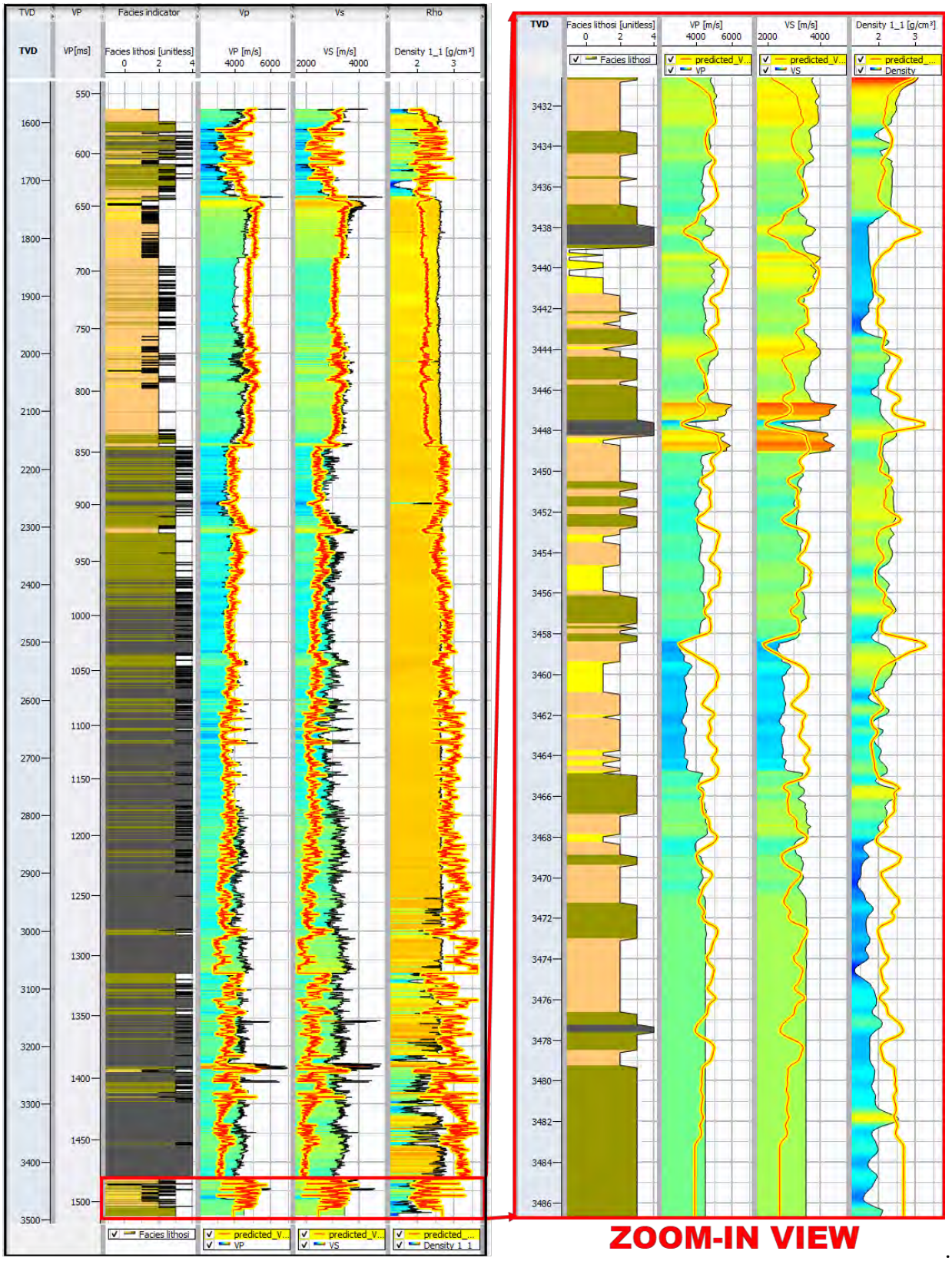

Figure 5.2: A comparison of modelled logs versus recorded logs of Miano-02 well s showing facies Vp and VS wave velocities and density logs.

5.4 Cross-Plots analysis:

The results from the cross plots are elaborated in the following points separately:

- **P-wave Velocity vs Bulk Density:** The cross plot of P-wave velocity vs Bulk density is a fundamental tool for understanding the relationship between seismic properties and rock density. In this study, the results from this cross plot revealed several important insights:
  - Correlation Between Vp and Rho: The cross plot likely showed a positive correlation between Vp and Rho, indicating that as density increases, P-wave velocity also tends to increase. This is a common trend in rock physics and is associated with the stiffness of rocks.
  - Clustering and Variability: Clusters or groupings of data points on the cross plot would have indicated distinct lithological or compositional trends within the Lower Goru Formation. Variability within these clusters may reflect differences in rock types or fluid content.
  - Model Validation: The strong alignment between the modeled Vp and the actual well-log data points would have served as a validation of the rock physics models. Any deviations may suggest areas where the models require refinement.
- **Porosity vs P-wave Velocity:** The cross plot of porosity vs P-wave velocity is crucial for understanding how porosity affects seismic properties. In this context:
  - Porosity-Velocity Relationship: The cross plot would have revealed whether there was an inverse relationship between porosity and P-wave velocity, as is often the case. As porosity increases, P-wave velocity typically decreases due to the presence of fluid-filled pores.
  - Hydrocarbon Indicators: Any significant deviations from the expected porosity-velocity trend could indicate the presence of hydrocarbons. This is because hydrocarbons, being less dense than water, can lead to anomalously low velocities in porous rocks.
- **Acoustic Impedance VS Ratio of P-wave to S-wave Velocity:** The cross plot of acoustic impedance vs the ratio of P-wave to S-wave velocity provides insights into the rock's impedance contrast and elastic properties:
  - Impedance Contrast: The cross plot would have illustrated variations in impedance contrast within the Lower Goru Formation. A clear pattern or clustering of data points may suggest changes in lithology or fluid content.
  - Identification of Fluid Substitution Effects: In cases where hydrocarbons are present, deviations from the expected trend in the Ip vs Vp/Vs cross plot may indicate fluid substitution effects. The presence of hydrocarbons typically results in lower impedance and velocity ratios.

- **P-wave Velocity vs S-wave Velocity:** The cross plot of P-wave velocity vs S-wave velocity is essential for understanding the mechanical properties and elastic behavior of rocks:
    - Elastic Moduli Relationships: This cross plot helps assess the relationship between P-wave and S-wave velocities, which, in turn, reflects the rock's elastic moduli. A linear trend would indicate consistent elastic properties, while deviations may suggest anisotropy or variations in rock stiffness.
    - Identification of Rock Types: Clusters of data points in the cross plot may indicate distinct rock types or lithological variations within the Lower Goru Formation. The angle of the trend line relative to the x-axis could provide insights into the rock's mechanical anisotropy.

In summary, these cross plots serve as valuable tools for understanding the relationships between different seismic properties and rock characteristics within the Lower Goru Formation. They provide insights into lithology, porosity, fluid content, and mechanical properties, helping to refine rock physics models and enhance our understanding of the subsurface reservoir features.

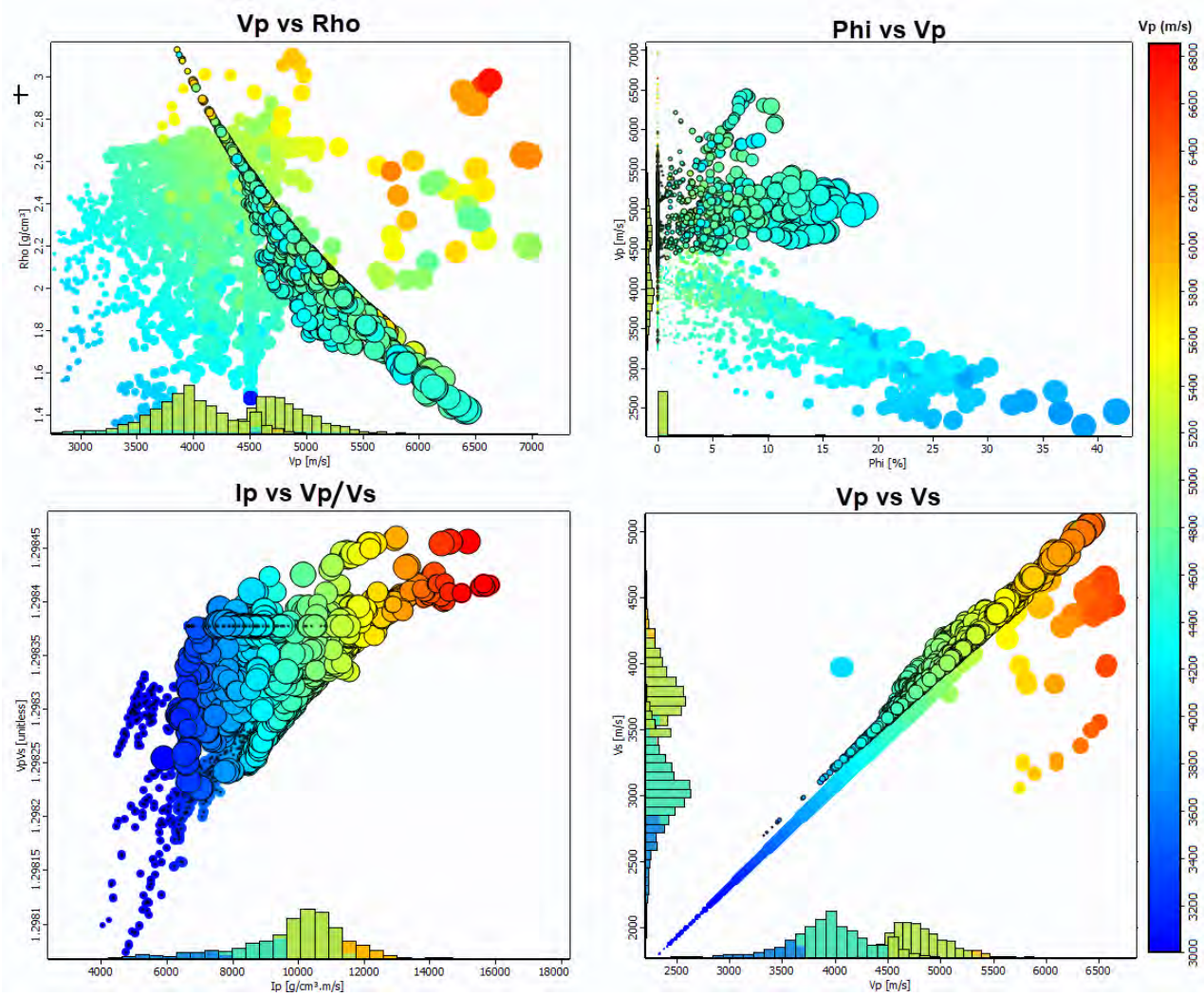

Figure 5.3: Cross plot comparison of various properties a). Vp vs Rho b). Phi vs Vp c). Ip vs Vp/Vs d). Vp vs Vs. Dots with black outline show predicted data while without any outline show recorded data. Predicted data show more convergence and uniform distribution. Dots are colored based on Vp values (see legend).

5.5 Error analysis from Cross-Plots

The results of the cross plots of modelled versus measured elastic attributes (Rho, Vp, and Vs) estimated by the petro elastic model (PEM), in the context of the previous discussion:

- **Predicted Rho versus Measured Rho:** This cross plot of predicted density (Rho) versus measured density provides essential insights into the accuracy and reliability of the petroelastic model's predictions. In the context of the previous discussion:
  - Convergence and Uniform Distribution: The statement that the data shows "convergence and uniform distribution" suggests that the predicted Rho values closely match the measured Rho values. In other words, the Petro elastic model accurately estimates density, and there are no significant systematic errors or biases.
  - Robust Model Validation: The convergence of predicted and measured Rho values is a crucial indicator of the model's robustness and validity. It demonstrates that the model

successfully captures the relationship between rock properties (e.g., mineral composition, porosity) and density, as observed in the well-log data.

- **Predicted Vp versus Measured Vp:** The cross plot of predicted P-wave velocity (Vp) versus measured Vp provides insights into the model's ability to predict seismic velocity accurately:
  - Convergence and Uniform Distribution: Similar to the Rho cross plot, the convergence and uniform distribution of data points suggest that the predicted Vp values closely match the measured Vp values. This alignment indicates that the Petro elastic model effectively captures the factors influencing P-wave velocity within the Lower Goru Formation.
  - Reliability of Velocity Predictions: The agreement between predicted and measured Vp values reaffirms the reliability of the Petro elastic model in predicting seismic velocities. This is critical for accurately characterizing subsurface geological properties and behavior.
- **Predicted Vs versus Measured Vs:** The cross plot of predicted S-wave velocity (Vs) versus measured Vs provides insights into the model's capability to estimate shear wave velocities:
  - Convergence and Uniform Distribution: Once again, the convergence and uniform distribution of data points imply that the predicted Vs values align closely with the measured Vs values. This indicates that the Petro elastic model (PEM) effectively considers the rock's mechanical properties and accurately predicts shear wave velocities.
  - Mechanical Properties Representation: The agreement between predicted and measured Vs values underscores the model's ability to represent the mechanical properties of rocks within the Lower Goru Formation. This is crucial for understanding the sub surface's elastic behavior and anisotropy.

In the context of the previous results, these cross plots provide compelling evidence of the Petro elastic model's accuracy and reliability. The convergence and uniform distribution of data points across all three attributes (Rho, Vp, and Vs) validate the model's ability to capture the intricate relationships between rock properties and seismic attributes. This validation enhances confidence in the rock physics models' applicability in predicting seismic properties within the specific geological environment of the Lower Goru Formation, supporting further analysis and decision-making in exploration and production activities.

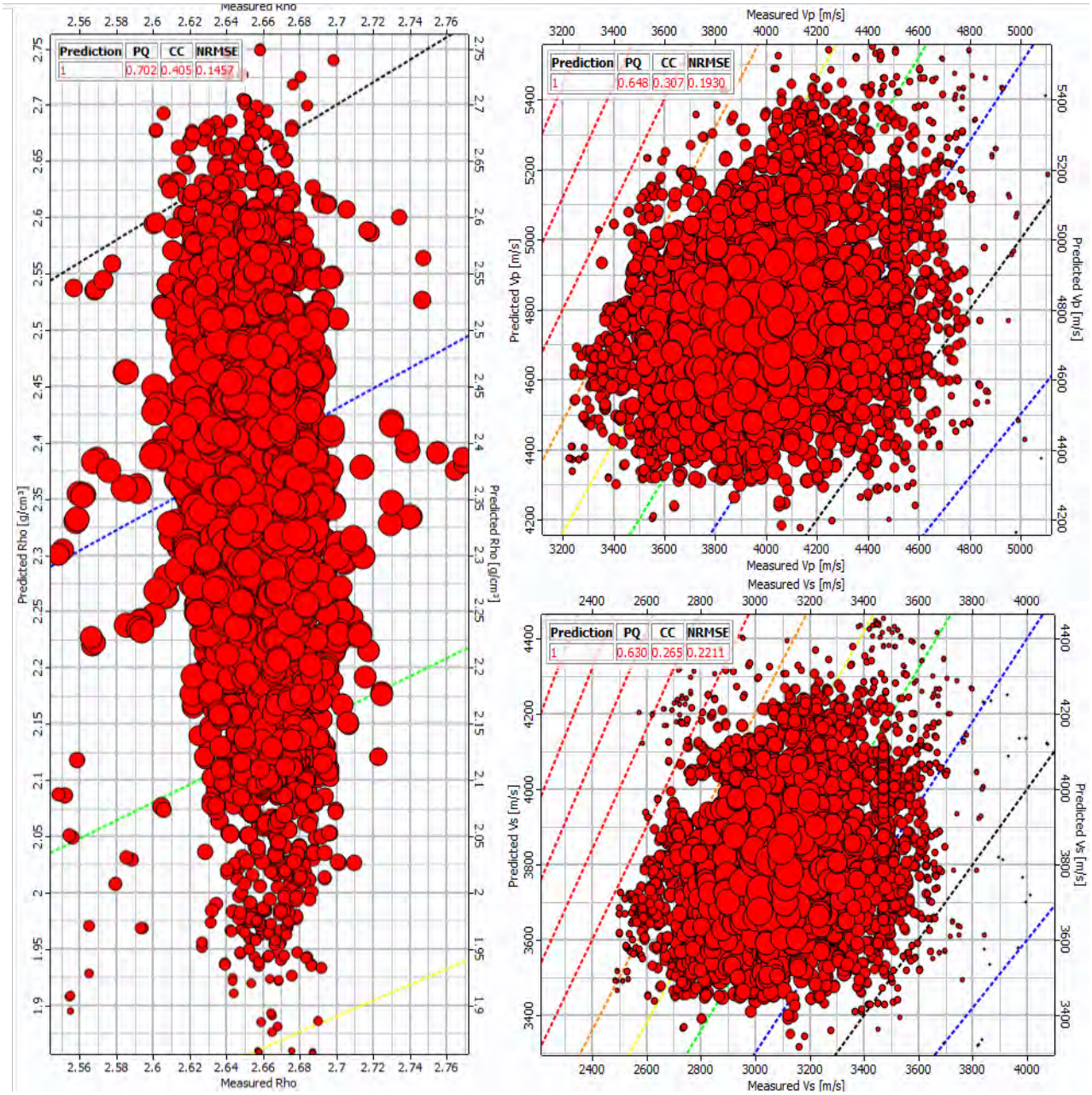

Figure 5.4: Cross plots of modelled versus measured elastic attributes estimated by Petro elastic model a). Predicted Rho versus measured Rho b). Predicted Vp versus measured Vp c). Predicted Vs versus measured Vs. Data show convergence and uniform distribution in the Lower Goru zone with producing gas sands.

5.6 Simulation Results

The results of the simulation and modeling efforts within the Lower Goru Formation in the Miano Gas Field, as described in the provided information, are indeed noteworthy. They represent a substantial contribution to understanding the behavior of seismic waves and the characterization of subsurface reservoir features. Let's delve into these results and their significance:

- **Validation of Rock Physics Models:** The successful validation of rock physics models is a critical achievement. The fact that these models purified log responses and accurately predicted the S-wave log underscores their reliability and applicability.
- **Insights into Seismic Wave Behavior:** The primary goal of the study was to gain insights into the underlying intricacies influencing seismic wave behavior. The results indeed provide valuable insights into how various rock properties affect seismic attributes, such as P-wave velocity (VP), S-wave velocity (VS), and density.
- **Alignment with Geological Parameters:** The consistent sample distribution pattern observed in the models, closely matching the geological parameters of the Lower Goru Formation, is a remarkable finding. This alignment reinforces the trustworthiness of the models as forecasting tools tailored to the specific geological setting.
- **Robust Correlations in Cross plots:** The exceptionally robust correlations revealed in cross plot research emphasize the intricate relationships between rock properties and seismic reactivity. This is valuable information for understanding how different geological factors influence seismic attributes.
- **VP Convergence with Actual Log Data:** The significant convergence of VP values in the models with actual log data, particularly in areas with increased porosity and fluid content, is a significant observation. It demonstrates the model's capability to capture the impact of porosity and fluid content on seismic velocity.
- **Complex Heterogeneity and Anisotropy:** The recognition of occasions where the model understated VP indicates the presence of complex underlying heterogeneity and anisotropy. This highlights the need to consider geological complexities that may not be fully represented by simplified models.
- **Consistency with Lithology and Density:** The remarkable agreement between density logs and modeling results confirms the strong link between lithology and density in the Lower Goru sands. This finding is crucial for accurately characterizing rock properties.
- **Enhanced Understanding of Reservoir Features:** The rigorous validation of the rock physics models significantly improves their applicability. This enhancement is particularly valuable for understanding the subsurface reservoir features within the Lower Goru Formation, a critical aspect of hydrocarbon exploration and production.

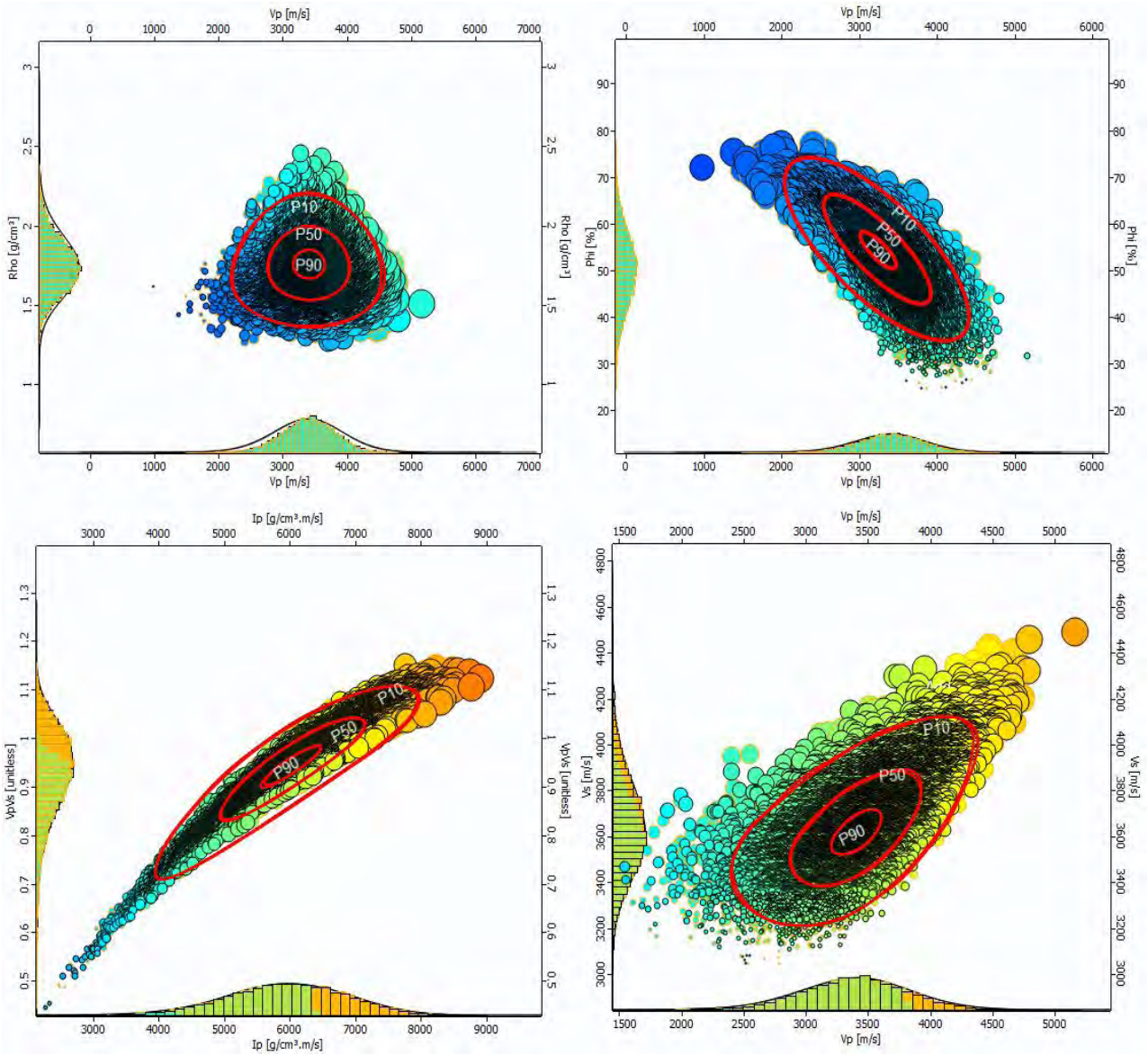

Figure 5.5: Monte Carlo Simulations for various properties using cross plot analysis. **a**). Vp versus Rho **b).** Rho versus Phit **c).** Ip versus Vp/Vs **d).** Vp versus Vs. P90, P50 and P10 shows 90%, 50% and 10% probabilities respectively. Simulated data will be used as training dataset for Geostatistical inversion.

5.7 Conclusions

The rock physics modeling and simulation efforts within the Lower Goru Formation in the Miano Gas Field have yielded significant insights. These efforts aimed to enhance the understanding of seismic wave behavior and improve reservoir characterization. One of the most crucial outcomes of this study is the successful validation of rock physics models, which have been proven to purify log responses and accurately predict the S-wave log. The primary objective of this research was to gain insights into the intricate factors that influence seismic wave behavior, and the results have provided valuable understanding in this regard. Notably, the rock physics models have exhibited a consistent sample distribution pattern that closely mirrors the geological parameters observed in the Lower Goru Formation. This alignment has reinforced the trustworthiness of these models as forecasting

tools, tailored specifically to the geological setting under consideration. The cross plot research conducted as part of this study has revealed exceptionally robust correlations between various rock properties and seismic reactivity, highlighting the complex relationships that exist in the subsurface. A significant finding is the convergence of predicted P-wave velocity (VP) values with actual log data, particularly in areas with increased porosity and fluid content. However, occasional discrepancies have been observed, indicating the presence of complex underlying heterogeneity and anisotropy that are not fully represented by simplified models. The research has identified parallel patterns in S-wave velocity (VS) values, with minimal variances linked to the mechanical properties of the rocks. Additionally, density logs have shown remarkable agreement with modeling results, affirming the strong link between lithology and density in the Lower Goru sands. The rigorous validation of the rock physics models significantly enhances their applicability in understanding the Lower Goru Formation's subsurface reservoir features. These validated models are poised to be valuable tools in further analyses, such as Geostatistical inversion within the Miano Gas Field, providing more accurate reservoir characterization. In summary, the results of this study represent a substantial contribution to the field of subsurface exploration and reservoir characterization, underscoring the importance of considering geological complexities in seismic modeling and their impact on hydrocarbon exploration and production activities.

CHAPTER #06

6. Seismic Inversion

6.1 Introduction:

Geoscientists have used seismic inversion approaches for almost four decades, as described by Hampson and Russell in 1991. Seismic inversion's major goal is to comprehend subsurface structures by studying the correlations between reflecting interfaces and amplitude recorded on a line (Barclay et al., 2008). Inversion techniques convert the seismic interpreter's temporal reflectivity images into the geologist's depth perspective. This transformation is accomplished by including relevant constraints such as Earth's velocities, which are useful for reservoir characterization (Maulana, 2016). The work at hand, while appearing easy at first glance, is actually rather complex, as the various procedures of seismic data processing and collecting play a crucial role in this context. The primary advantage of using this technology is the seismic coverage it gives, which may cover huge areas both above and below the Earth surface. Especially, this is true for the large-scale 3D seismic surveys that are now routinely acquired for geological research. As a processing tool in reservoir characterization, seismic inversion is extremely important. According to Lloyd and Margrave (2011)'s scientific study, it is clear that the geological features under examination are critical.

In seismic forward modelling, we use a practice known as synthetic seismogram production. This entails multiplying velocity and density logs an impedance log production. Reflectivity series is then generated from this log. After that, the reflectivity series is convolved with a theoretical or extracted wavelet, yielding an estimate of the seismic response within a seismic sector. To counterbalance this arrangement, a process of inversion is initiated, beginning with a trace obtained from a seismic segment. It should be noted that this trace can only be used as a rough approximation to the synthetic seismogram. The forward technique has a high degree of certainty, but the inverse regression procedure can produce numerous feasible solutions for the acoustic impedance log. This is why geologists argue that inversions are never infallible, or as they are commonly known, "push-button" inversions.

The incorporation of these categorizations also leads to the development of supplementary Geoscientific methodologies that can be used to address the inversion challenge (Wang, 2003). The set of objectives to be achieved, as well as, in some cases, the properties of the subsurface medium, are key determinants in selecting the appropriate methodology. We used model-based inversion as one of the procedures and workflows for post-stack inversion in this study.

6.2 Model Based Inversion

This inversion algorithm works on the fundamental principles of convolution. The traces are formed as a result of the convolving of a reflectivity model from subsurface medium with a wavelet (Figure 6.1 & 6.2) along with the incorporation of the seismic noises (Maurya and Sarkar, 2016).

$$\text{Seismic trace} = \text{Wavelet} * \text{RC} + \text{Seismic Noise} \tag{6.1}$$

If this seismic noise does not correlate with seismic data, equation 6.1 can be used to estimate the subsurface reflectivity pattern. The phenomenon can be accurately described by a linear equation.

$$Z = V * \rho, \tag{6.2}$$

$$r_i = \frac{Z_{i+1} - Z_i}{Z_{i+1} + Z_i}, \tag{6.3}$$

$$AI_N = AI_1 exp\left(\sum_{i=1}^{n} r_i\right), \tag{6.4}$$

Where, AI_1 indicates the acoustic impedance of the uppermost layer, whereas AI_N represents the acoustic impedance the N-th layers. Furthermore, r_i signifies the reflection coefficient of the *i*-th layer's. When the value of r_i is smaller than 0.3, this equation is effective in a variety of real applications. The equations presented here are the most commonly used formulas in the practice of recursive inversion for the purpose of converting amplitudes to impedances, as explained by Berteussen and Ursin in their foundational work published in 1983. In geoscience, kriging interpolation is used to estimate the constraints present in the seismic cube, resulting in a low-frequency model. Acoustic impedance is rarely measured in well logs. These calculations are frequently based on sonic and density logs. Ferguson and Margrave's 1996 model-based inversion workflow includes the following procedures:-

- The acoustic impedances at the well locations are calculated using log data.
- Ensure the strategic placement of markers designating the borders of geological formations on the seismic section, boosting our understanding of the geological composition for the aim of building correct models in conjunction with nearby boreholes.
- Create a seismic section that highlights the interpreted horizons and wells, then interpolate the first acoustic impedance model using the specified parameters. Construct the basic impedance model using certain block sizes.
- The seismic data was used to generate the statistical wavelet.
- Convolve this wavelet with the Earth's reflection coefficient (RC) to construct a synthetic seismic trace. Certain characteristics of the extracted seismic section trace may vary.

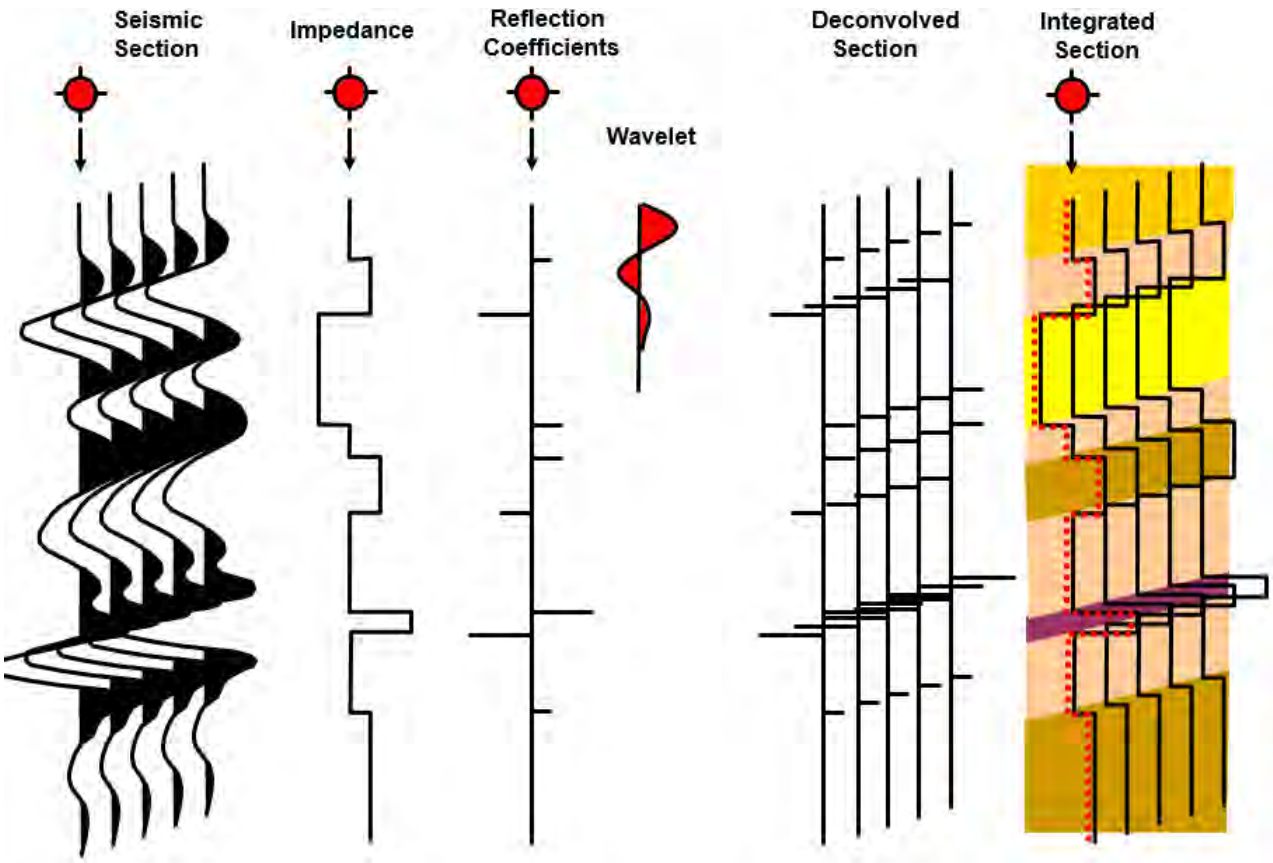

Figure 6.1: Schematic diagram of a Model-Based Inversion Procedure (Nasir et al., 2007).

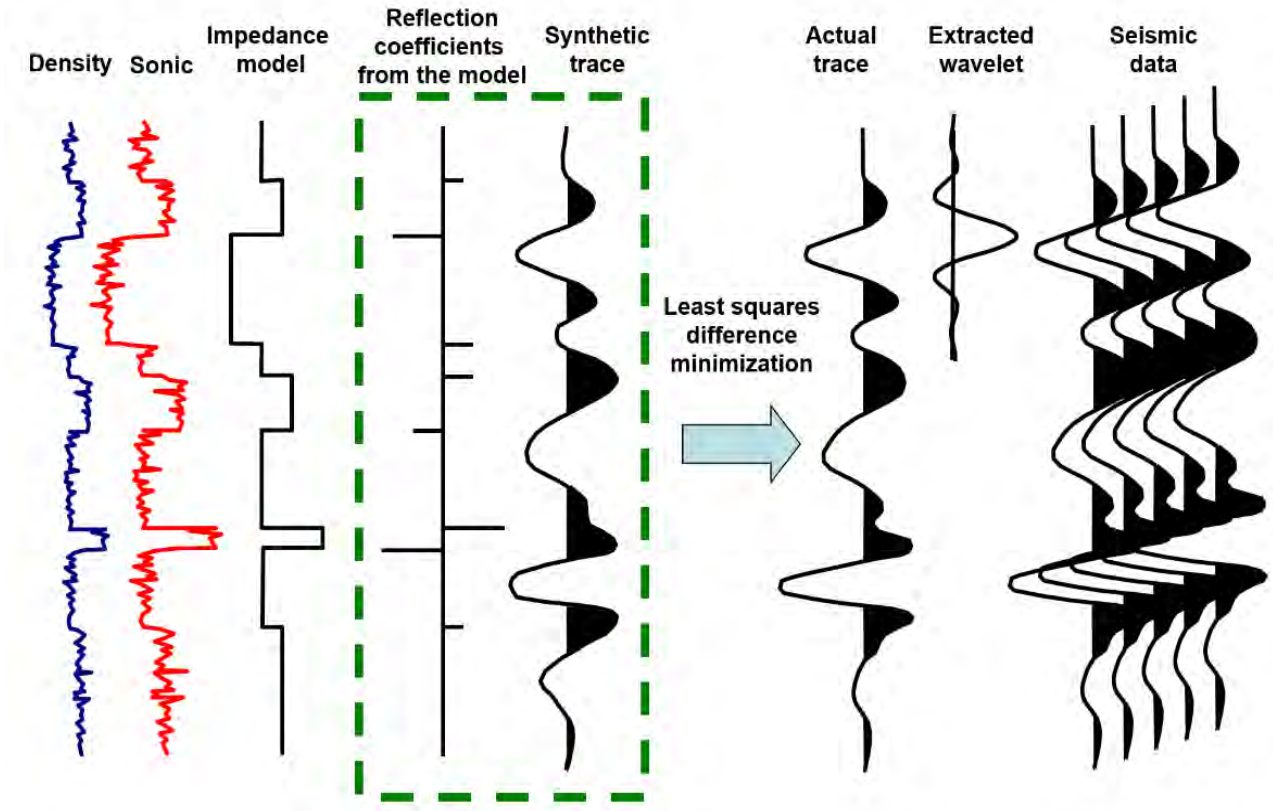

Figure 6.2: Convolution model for forward seismic trace generation (courtesy of CGG).

Following that, the Least Squares criterion is used to minimize the variance between the original Geological data and the data that has been modeled. Examine the misfit function for the synthetic seismic trace and the geological section's actual seismic trace. To reduce the error %, either the block sizes or the amplitudes could be adjusted. Step 7 should be repeated to achieve the smallest misfit function between the two traces. As stated by Maurya and Singh (2015), continue the geological processes till the desired goal is reached. Figure 6.4 shows the results of inversion analysis.

The seismic-to-well tie for the model-based inversion that was performed on the Miano-02 well serves as an essential step in the validation process for our efforts to characterize the subsurface. We are able to successfully establish a vital connection between the seismic data and the reality of the subsurface environment by contrasting the inversion results with the actual well data from Miano-02. This relationship not only validates the precision and dependability of our inversion method, but it also offers critical insights into the geological and Petrophysical characteristics of the Lower Goru Formation. This validation process, in effect, ensures that our model-based inversion properly depicts the subsurface. This enables us to make educated conclusions with a high degree of confidence regarding reservoir characteristics, porosity, fluid content, and lithology. This seismic-to-well tie helps bridge the gap between geophysical data and ground reality, which, in the end, allows us to have a better understanding of the reservoir and allows us to develop resource extraction tactics that are more effective.

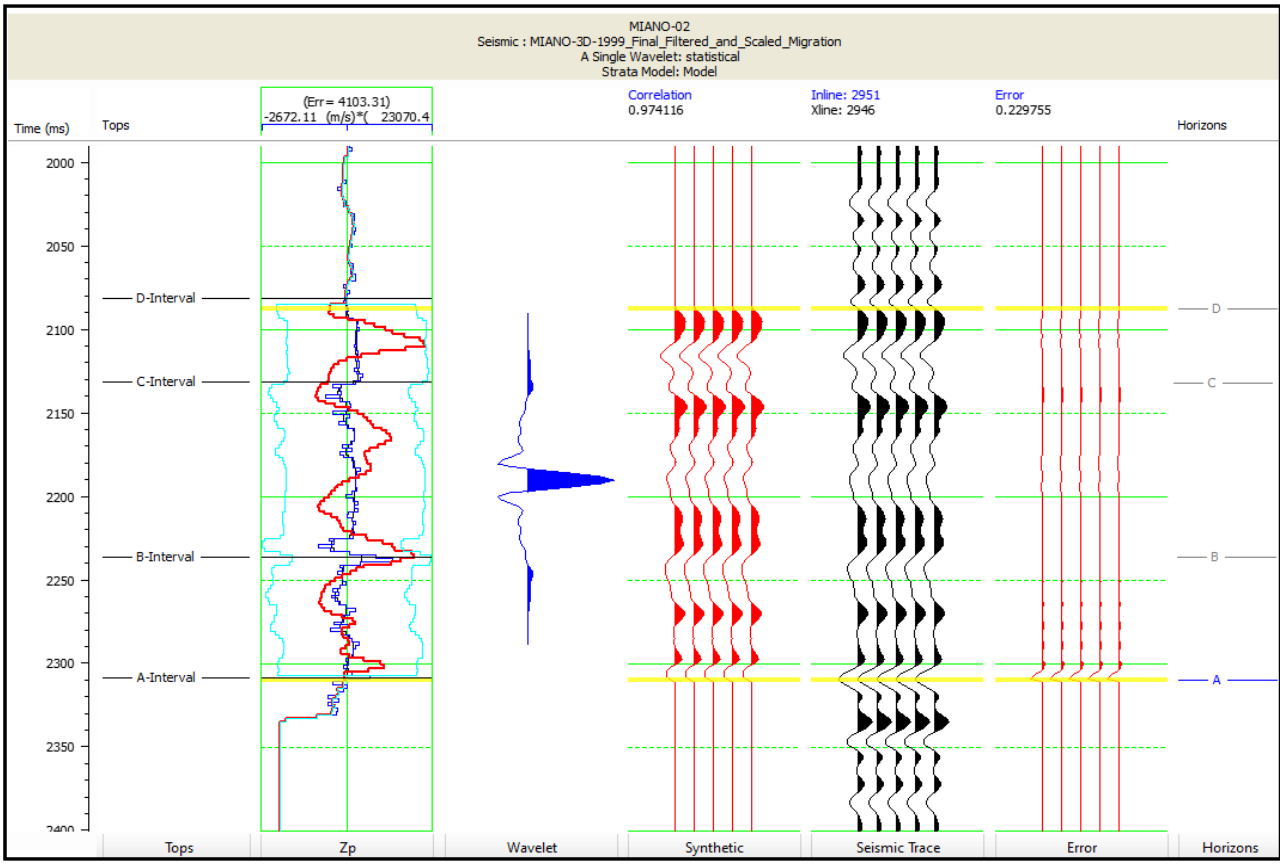

Figure 6.3: Correlation of strata model to seismic data

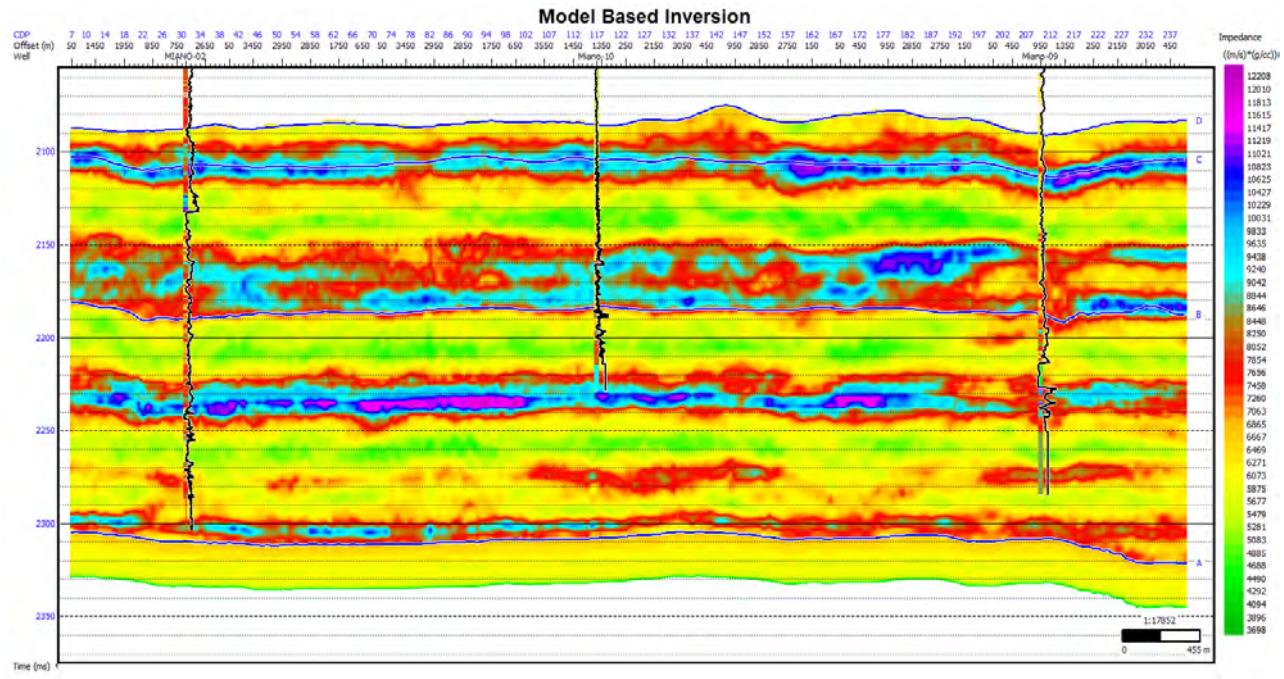

Figure 6.4: Model Based Inversion results shown on a composite line passing through all wells.

6.3 Geostatistical Stochastic Inversion (GEOSI)

Stochastic seismic inversion enhances the reservoir model's accuracy by integrating 3D seismic interpretation with Petrophysical properties. While structural seismic interpretation informs

reservoir model construction, incorporating 3D populated Petrophysical parameters remains less common. This is primarily due to challenges like limited 3D dataset availability, insufficient vertical resolution for precise property models, and difficulties linking seismic data quantitatively to reservoir properties (Rowbotham et al., 2003). The utilization of 3D seismic data can alleviate the initial shortcoming by linking seismically derived impedance volumes to reservoir attributes like porosity (φ), addressing the second challenge.

6.3.1 Seismic Resolution

It is more difficult to resolve restricted vertical resolution in reservoir property models. Stochastic seismic inversion, such is the method developed by Gunning and Glinsky (2003), increases the vertical resolution of 3D reservoir property models. This method uses precise 3D seismic integration and well-log data to construct geologically possible 3D realizations of P-impedance, engineering parameters, and lithology (Rutai et al., 2016). While log data has strong vertical resolution, due to its high vertical and low spatial resolution properties, it lacks sufficient horizontal resolution. Seismic data, on the other hand, has great areal resolution but lower vertical resolution (depending on seismic frequency and reservoir velocity). These records are effectively merged by stochastic seismic inversion for accurate subsurface imaging and characterization (Marion et al., 2000).

Stochastic seismic inversion yields high-resolution 3D volumes ideally suited for detailed property modeling. Seismic data provides areal resolution, while log data contributes vertical resolution. The typical stochastic inversion achieves a vertical resolution of around 1-2 meters, fitting the scale required for Petrophysical reservoir property modeling, including porosity (Rowbotham et al., 2003b). This process enhances reservoir projection, showcasing the integrated strategies as shown in Figure 6.5.

By incorporating well and geologic control into stochastic inversion, geophysicists can gain a profound understanding of subsurface structures and make informed exploration and production decisions (Latimer et al., 2000). The stochastic inversion approach crafts a consistent and quantitative reservoir representation by amalgamating data from all available measurements (Taner, 2001). Geostochastic inversion (GeoSI) employs a systematic workflow, as depicted in Figure 6.5, which aids in generating a unique representation of the reservoir.

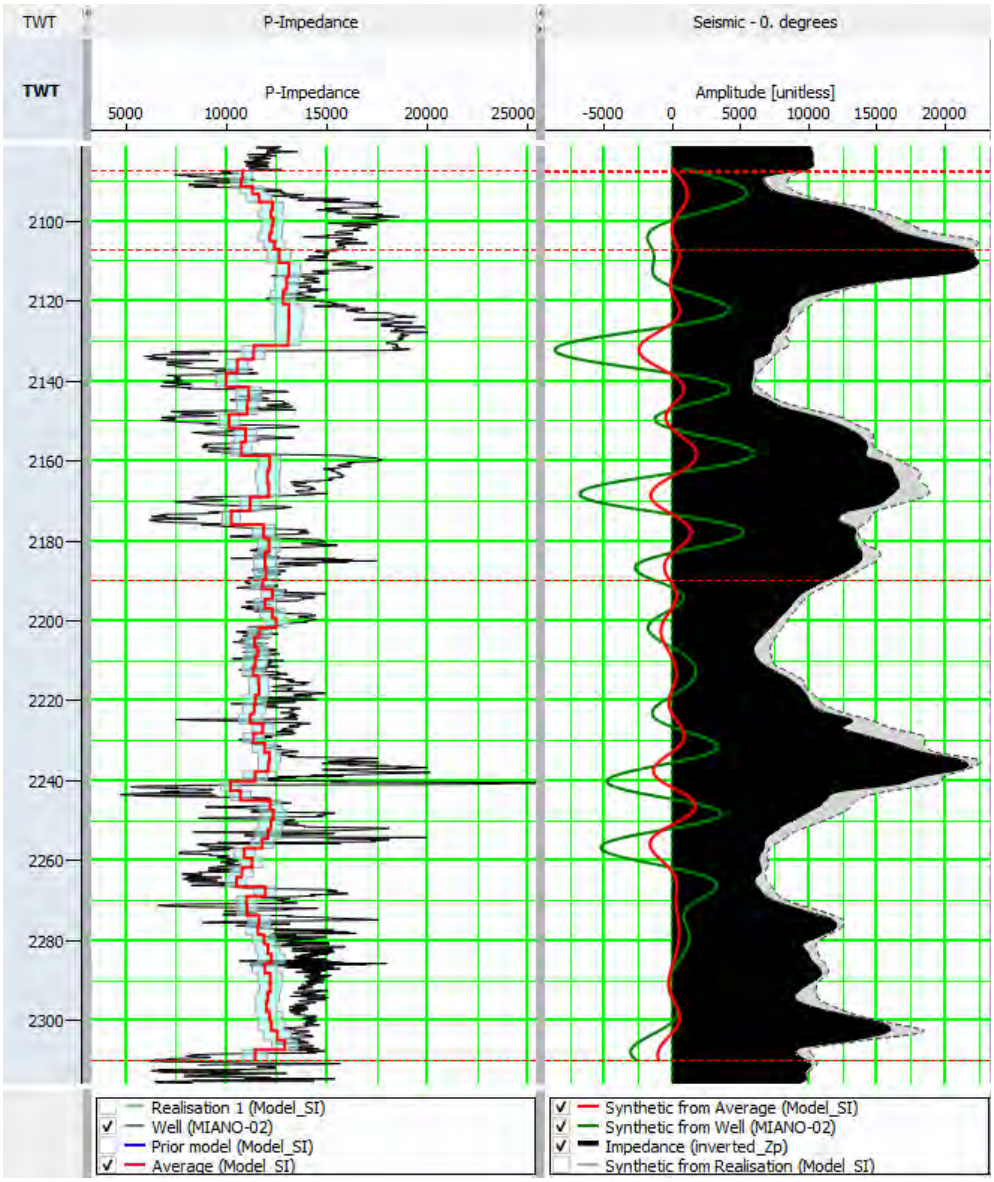

Figure 6.5: Up scaling of well logs to compare and correlate to seismic scale.

6.3.2 Low Frequency Model

GeoSI commences like other inversion methods, establishing correlation between well and seismic data. The Strata Model, akin to the Low Frequency Model (LFM), emerges from an inversion process. Seismic horizons are identified using interpolation, and low frequency Z_p, Z, and p models are constructed while maintaining structural tendencies. LFMs play a crucial role in subsequent stochastic inversion steps.

6.3.3 Prior Model (SI Model)

Unlike conventional inversion where the initial model incorporates well logs across seismic volumes, GeoSI requires a previous model with specified characteristics and seismic data limitations. A high-resolution stratigraphic grid is established (Figure 6.6), incorporating

Petrophysical characteristics for each stratum. A stratigraphic geo-cellular grid with a layer thickness of 0.1 ms accommodates high resolution to account for fluctuating thickness and depositional trends.

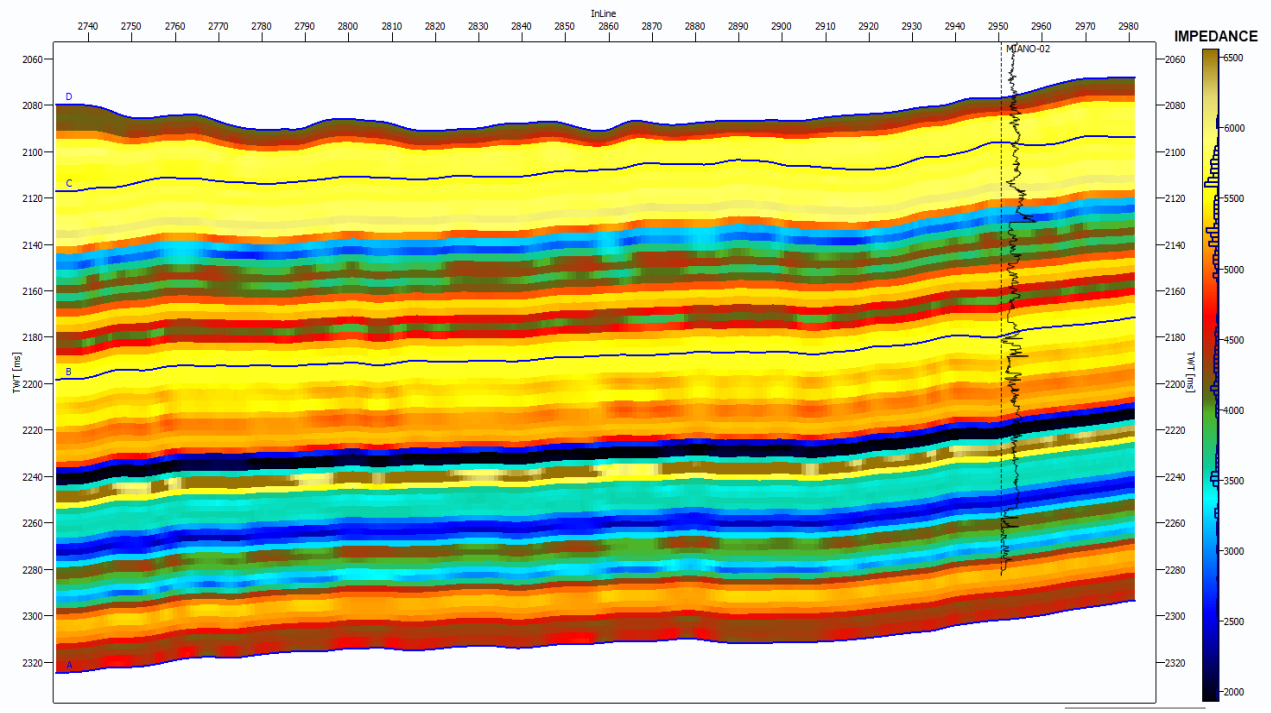

Figure 6.6: Initial model build for Geostatistical inversion build on basis of well logs.

6.3.4 Variogram Modelling

Variograms assess spatial continuity and changes in phenomena across regions. In oil and gas exploration, variograms analyze sparse well data and dense seismic data, aiding in interpolation through techniques like Kriging and Co-Kriging. These tools provide insights into lithological distribution and changes, guiding reservoir characterization and drilling direction.

Vertical and Horizontal Variograms

GeoSI employs variogram models to characterize spatial continuity both vertically and horizontally. Vertical variograms control well log data, while horizontal variograms use seismic data to capture structural and stratigraphic variations. Vertical variogram analysis shows lithological variations and stratigraphic trends, while horizontal variograms enhance understanding of lateral lithology and reservoir characteristics.

Variograms can be represented using functions like spherical, exponential, Gaussian, power, cubic, and stable. For GeoSI, the exponential function (equation 6.1) aptly characterizes structural and thickness changes in the Miano Gas Field dataset. Variogram parameters, including sill, nugget, and range, have been modelled for each layer.

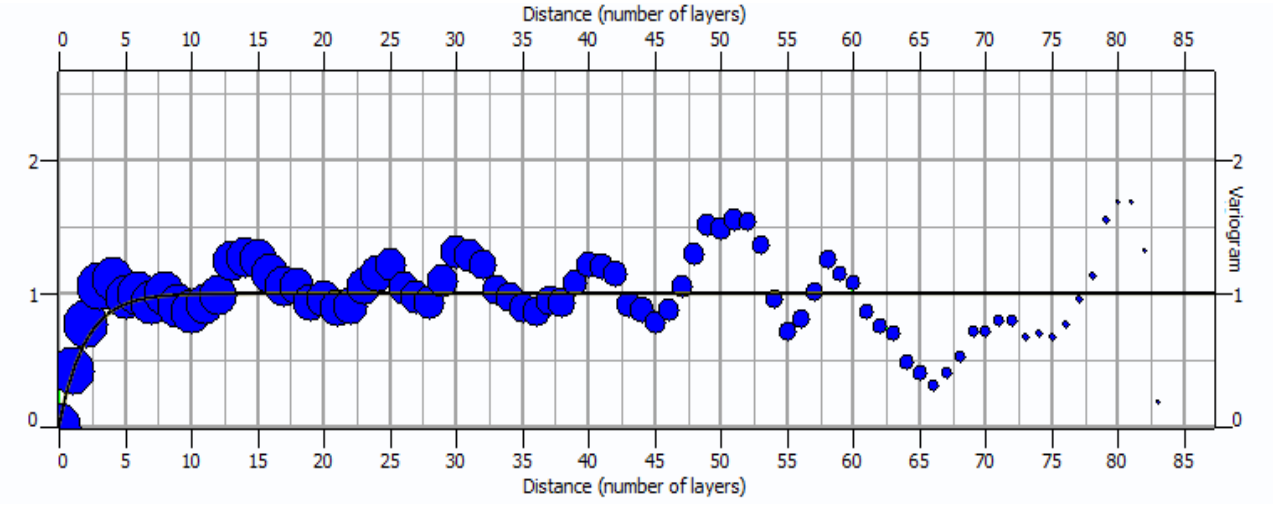

Figure 6.7: Variogram analysis done on Miano-02 well.

6.3.5 Wavelet

Selecting a suitable wavelet is pivotal for successful inversion. Wavelet extraction involves stable wavelet extraction from seismic traces with reliable reflection qualities, ensuring consistency between dominant frequency and target layer's wavelet, and maintaining minimal phase and spectral similarity. Single-well wavelets extracted through the seismo-statical approach are averaged and calibrated for inversion.

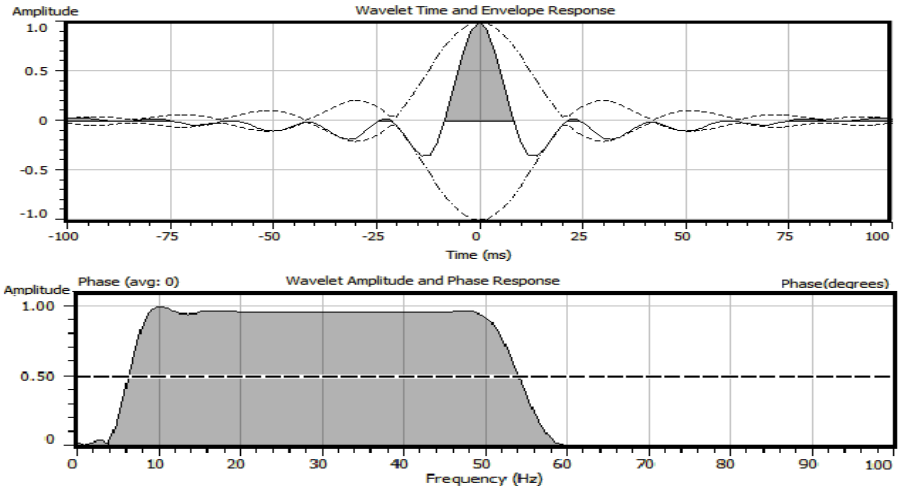

Figure 6.8: Statistical wavelet extracted used of Geostatistical inversion.

6.3.6 Posterior Model and Gas Sand Probability

Analyzing parameters and prior models at well locations precedes inversion across the volume. Bayesian classification evaluates ID inversion analysis, aiming for high correlation and minimal deviation. Gas Sand Probability gauges the likelihood of gas-containing rock layers, facilitating hydrocarbon reservoir identification.

Stochastic seismic inversion through the GeoSI technique combines seismic and well log data for precise reservoir characterization. This approach's multifaceted workflow effectively integrates various data sources, enhances accuracy, and informs better reservoir development decisions.

6.4 Results:

Seismic inversion, a crucial tool in the field of subsurface reservoir characterization, has been employed in this study to gain insights into the reservoir sands of the B-Interval within the Lower Goru Formation. The results obtained from two different inversion algorithms, the model-based approach and the Geostatistical inversion, have provided valuable information about the subsurface properties. In this section, we will delve into the details of these results and draw meaningful conclusions regarding the reservoir characteristics.

The seismic inversion results obtained from both the model-based algorithm and the Geostatistical inversion have demonstrated a commendable level of consistency. This consistency underscores the reliability of the inversion process and the robustness of the algorithms used. It is essential to note that such consistency is a fundamental requirement in subsurface reservoir characterization, as it forms the basis for making informed decisions regarding resource exploration and extraction.

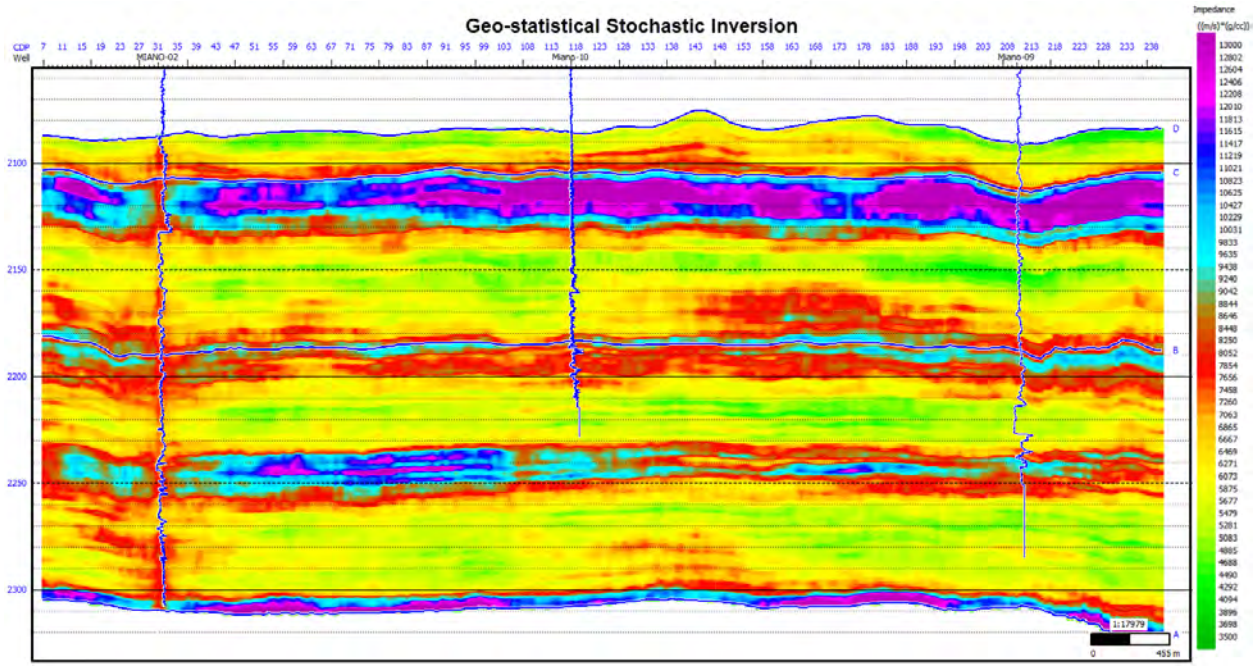

Figure 6.9: Geostatistical inversion results shown on a composite line passing through all wells.

While both inversion algorithms have yielded consistent results, the Geostatistical inversion stands out for its ability to provide higher resolution and a more realistic depiction of the reservoir sands within the B-Interval of the Lower Goru Formation. This enhanced resolution is of significant value

as it allows for a finer understanding of the subsurface properties. In practical terms, higher resolution translates to better-informed decision-making, especially when it comes to well placement and drilling strategies.

One of the key findings in our seismic inversion results is the notable variation in the thickness of reservoir sands within the B-Interval. The upper zone exhibits a lower thickness, while the lower zone displays a higher thickness of reservoir sands. This observation is in close alignment with the Petrophysical results, which independently confirm the higher sand thickness in the lower zone. Such concordance between seismic inversion and Petrophysical data is highly reassuring, as it corroborates the accuracy of our findings.

The map view of our inversion results provides additional insights into the horizontal distribution of reservoir impedances. Figure 6.10 (a) displays the results from the model-based algorithm, while (b) and (c) present the outcomes of the Geostatistical inversion with varying numbers of realizations. Notably, the Geostatistical inversion offers a superior level of continuity and clarity in representing the horizontal distribution of reservoir impedances. This level of detail is immensely valuable, as it aids in pinpointing specific areas of interest for resource extraction.

However, it is essential to acknowledge that as the number of realizations in the Geostatistical inversion increases, the data prediction becomes more biased, and the predictions themselves become less reliable. This phenomenon is a crucial consideration in the interpretation of our results. It highlights the need for a balanced approach when employing Geostatistical inversion, where the number of realizations must be carefully chosen to optimize the trade-off between resolution and reliability.

Figure 6.10 (d) further enriches our understanding of the B-Interval's lower zone sand reservoir by presenting the porosity distribution. High porosity zones are indicative of better reservoir portions, and these zones align closely with the Petrophysical results. The porosity values obtained from the inversion process are in strong accordance with the independent Petrophysical data, further enhancing the credibility of our findings.

In conclusion, our seismic inversion results have provided valuable insights into the reservoir sands of the B-Interval within the Lower Goru Formation. The consistency between different inversion algorithms instills confidence in the reliability of our findings. However, it is the Geostatistical inversion that stands out for its enhanced resolution and ability to present a more realistic picture of the subsurface.

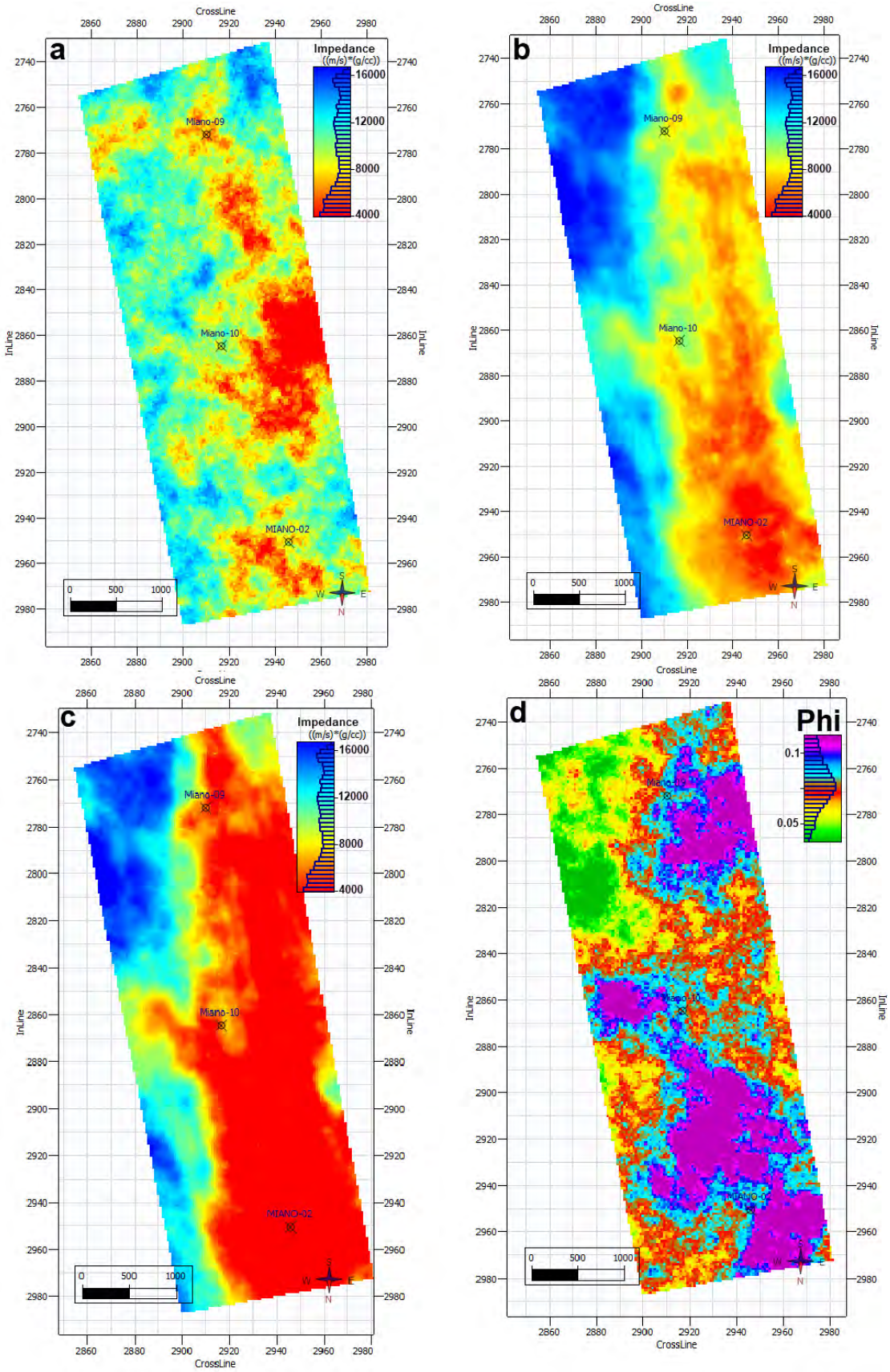

Figure 6.10: Comparison of seismic impedance maps on B-Interval sand layer time derived from (a) model based inversion versus (b & c) Geostatistical inversion (b) at 20 realizations and (c) 50 realizations. (d) Shows the porosity distribution along sand layer.

These results have significant implications for resource exploration and extraction. The ability to accurately identify variations in reservoir thickness and map the horizontal distribution of reservoir impedances is instrumental in optimizing well placement and drilling strategies. It empowers decision-makers with valuable information to maximize resource recovery while minimizing risks.

As we move forward, it is essential to continue refining our approach to Geostatistical inversion, striking a balance between resolution and reliability by carefully selecting the number of realizations. Additionally, the integration of seismic inversion results with other geological and Petrophysical data sources holds promise for further enhancing our understanding of subsurface reservoirs.

In summary, our seismic inversion results are a testament to the power of modern geophysical techniques in unraveling the complexities of the subsurface. They pave the way for more informed and effective resource exploration and extraction strategies, ultimately contributing to the sustainable development of our energy resources.

As we reflect on the results and conclusions of our study, several recommendations emerge to further enhance our understanding of subsurface reservoirs and optimize resource extraction. Firstly, it is advisable to conduct additional research to fine-tune the Geostatistical inversion process, finding the optimal balance between resolution and reliability. Moreover, ongoing data collection and integration efforts, including geological, Petrophysical, and production data, should be prioritized to create a comprehensive reservoir characterization framework. Additionally, the industry should invest in advanced computational resources and machine learning techniques to handle the increasing complexity of subsurface data analysis. Lastly, collaborative efforts between academia, industry, and regulatory bodies can facilitate knowledge sharing and best practices, ensuring responsible and sustainable energy resource management. By adhering to these recommendations and embracing technological advancements, we can pave the way for a more efficient, precise, and environmentally conscious approach to subsurface resource exploration and development.

6.4.1 Proposed location on base map for Future Drilling:

After review of our Inversion results the proposed location on the base map will be cross line 2936 and inline 2895 as shown in Figure 6.11 which has good reservoir characteristics and is recommended for drilling in future.

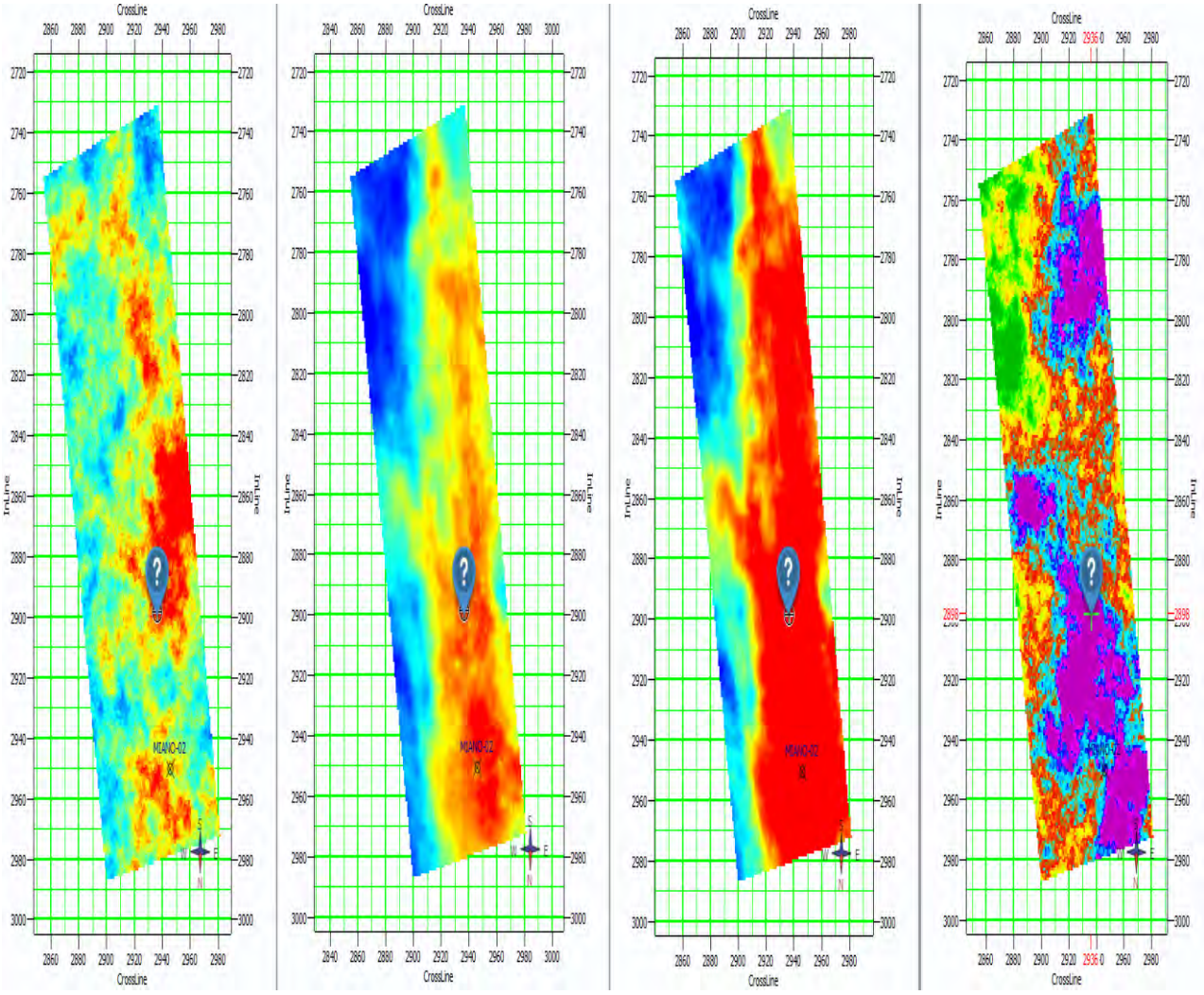

Figure 6.11: (Proposed location on base map with cross line 2936 and inline 2895 has good reservoir characteristics)

CHAPTER #07

Discussions

The investigation conducted in the Miano block, utilizing 3D post-stack seismic data and well log information, has yielded significant insights into the field's geology. This achievement was made possible through the application of advanced Geostatistical and rock physics modeling techniques. In particular, the study successfully determined the spatial distribution of a high porosity sand layer within the field, which holds great promise for hydrocarbon exploration.

These findings align with existing research and literature, providing strong support for their validity. The Miano block, characterized by planar-tilted fault blocks and half Grabens, particularly towards the Jacobabad-Khairpur High, has been recognized as a favorable prospect for hydrocarbon exploration by Jadoon et al. in their 2020 study. Moreover, the region is dissected by regional fault lines running from NW to SE (Asim et al. 2015; Kazmi & Jan 1977). Additional corroboration of the research findings comes from Naseer et al.'s work in 2017. They conducted attribute analysis on seismic data and performed inversion analysis, identifying the Lower Goru sand Intervals as prospective producing zones. This aligns seamlessly with the zones highlighted in this thesis. Furthermore, Khan's doctoral research in 2017, which involved seismic modeling, inversion analysis, and Petrophysical assessment, substantiates the potential of the B-Interval sands in this region. Khan's comprehensive analysis of geological structures and Petrophysical data further underscores the promise of these sands.

Additionally, research conducted on the overall basin, including depositional settings and sequence stratigraphy, by Ahmed et al. in 2004, Aadil et al. in 2011, and Toosy et al. in 2021, provides valuable context and background information for the findings in this investigation. In conclusion, the integration of multiple sources of information and the alignment with previous research strongly support the conclusions drawn from this study regarding the promising sand layers within the Lower Goru B-Interval in the Miano block.

The integration of rock physics modeling and seismic inversion techniques is crucial for the oil and gas sector to understand the hidden mysteries of the subsurface (Mukerji et al., 2011). The modeling of rock mechanics and seismic inversion work together to establish a powerful synergetic relationship, providing the foundation for accurately depicting underground oil and gas deposits. This approach utilizes mathematical and physical principles to represent subsurface rocks' influence on seismic waves and geophysical data, aiding resource development and understanding mineral densities (Miraj et al., 2021). The primary function of rock physics models is to establish correlations

between the physical properties of rocks and seismic features, which serves as guides in seismic inversion. These models improve the interpretation of seismic data within inversion algorithms, enabling correlations between subsurface properties with geological and Petrophysical occurrences. Seismic inversion, on the other hand, is the pinnacle of this modeling process, as it transforms seismic data into relevant subsurface rock properties. This computational technology is crucial in characterizing reservoirs by providing valuable insights into elusive features buried deep beneath the earth's surface. By determining the reservoir's lithology, fluid content, and porosity, it reveals its hidden characteristics. These methods offer a comprehensive analysis and responsible management of oil and gas resources, providing a more sustainable and informed approach to resource exploration and extraction.

Conclusions and Recommendations:

- There were no notable structural faults observed however several minor faults were not taken into account due to data limitations. So from Seismic Interpretation we have identified notable horizons include A-interval, B-interval, C-interval, and D-interval of Lower Goru formation which contain economic sand reservoirs and stratigraphic units.
- Two separate Petrophysical zones with distinct sand thicknesses have been identified, with Zone-I having a net pay thickness of roughly 30 metres and an effective porosity of 11.6%, and Zone-II of the C-interval having a net pay thickness of 17 metres and an effective porosity of 8%.
- Integration of rock physics models improved well log accuracy and enhanced shear wave predictions for inversion analysis with an accuracy of 85%.
- Inversion analysis revealed spatially low impedance and high porous areas possessing Gas, guiding prospect identification and help in field evolution.
- Geo-Statistical inversion yields geologically realistic results with improved resolution, as evidenced by clearer acoustic impedance maps compared to model-based inversion.
- A low impedance zone with high porosity was found southwest of the Miano-2 well. The point location on base map with cross-line 2936 and the inline 2895 is offered to have good reservoir characteristics and is being recommended for drilling based on this comprehensive study.

Overall, this investigation has advanced our knowledge of the Miano block's geology and hydrocarbon potential, marking a significant step in hydrocarbon exploration.

REFERENCES

- Aadil, N., & Sohail, G. M. (2011). Stratigraphic correlation and isopach maps of Punjab platform in middle Indus Basin, Pakistan. AAPG, Search and Discovery Article-10364, Tulsa.
- Abe, S. J., Olowokere, M. T., & Enikanselu, P. A. (2018). Development of model for predicting elastic parameters in 'bright'field, Niger Delta using rock physics analysis. NRIAG Journal of Astronomy and Geophysics.
- Adedeji, E. A. (2016). 3D Post-stack Seismic Inversion using Global Optimization Techniques: Gulf of Mexico Example.
- Ahmad, N., Fink, P., Sturrock, S., Mahmood, T., and Ibrahim, M. (2004). Sequence stratigraphy as predictive tool in lower goru fairway, lower and middle Indus platform, Pakistan. PAPG, ATC, 85-104.
- Ali, A., Alves, T. M., Saad, F. A., Ullah, M., Toqeer, M., & Hussain, M. (2018). Resource potential of gas reservoirs in South Pakistan and adjacent Indian subcontinent revealed by post-stack inversion techniques. Journal of Natural Gas Science and Engineering, 49, 41-55.
- Ali, M., Ma, H., Pan, H., Ashraf, U., & Jiang, R. (2020). Building a rock physics model for the formation evaluation of the Lower Goru sand reservoir of the Southern Indus Basin in Pakistan. Journal of Petroleum Science and Engineering, 194, 107461.
- Asquith, G., & Gibson, C. (1982). Basic well log analysis for geologists: methods in Exploration series. AAPG, Tulsa, Oklahoma.
- Asim*, S., Zhu, P., Naseer, T., Ahmed, S., Hussain, F., & Mudasir, M. (2015, July). Rock Physics modeling; attribute application and seismic inversion study in Miano, Lower Indus Basin of Pakistan. In Near-Surface Asia Pacific Conference, Waikoloa, Hawaii, 7-10 July 2015 (pp. 464-467). Society of Exploration Geophysicists, Australian Society of Exploration Geophysicists, Chinese Geophysical Society, Korean Society of Earth and Exploration Geophysicists, and Society of Exploration Geophysicists of Japan.
- Azeem, T., Chun, W. Y., MonaLisa, Khalid, P., Qing, L. X., Ehsan, M. I., ... & Wei, X. (2017). An integrated petrophysical and rock physics analysis to improve reservoir characterization of Cretaceous sand intervals in Middle Indus Basin, Pakistan. Journal of Geophysics and Engineering, 14(2), 212-225.
- Barclay, F., Bruun, A., Rasmussen, K. B., Alfaro, J. C., Cooke, A., Cooke, D., ... and Özdemir, H. (2008). Seismic inversion: Reading between the lines. Oilfield Review, Schlumberger, 20(1), 42-63.
- Berteussen, K. and Ursin, B. (1983). Approximate computation of the acoustic impedance from seismic data. Geophysics, 48(10):1351-1358.
- Bjørlykke, K., and Jahren, J. (2010). Sandstones and sandstone reservoirs. In Petroleum Geoscience (pp. 113-140). Springer, Berlin, Heidelberg.
- Bongajum, E. L., Boisvert, J., and Sacchi, M. D. (2013). Bayesian linearized seismic inversion with locally varying spatial anisotropy. Journal of Applied Geophysics, 88, 31-41.
- Burch, D. (2002). Log ties seismic to ground truth. The Geophysical Corner, 2, 26-29.
- Ellis, D. V., and Singer, J. M. (2007). Well logging for earth scientists (Vol. 692). Dordrecht: Springer.
- Jadoon, S. U. R. K., Lin, D., Ehsan, S. A., Jadoon, I. A., & Idrees, M. (2020). Structural styles, hydrocarbon prospects, and potential of Miano and Kadanwari fields, Central Indus Basin, Pakistan. Arabian Journal of Geosciences, 13, 1-13.
- Kearey, P., Brooks, M., and Hill, I. (2013). An introduction to geophysical exploration. John Wiley and Sons.
- Khan, M. A. (2010). Effects of human resource management practices on organizational performance–an empirical study of oil and gas industry in Pakistan. European Journal of Economics, Finance and Administrative Sciences, 24(157-174), 6.
- Khan, J. M., Moghal, M. A., and Jamil, M. A. (1999). Evolution of shelf margin and distribution of reservoir facies in early cretaceous of Central Indus Basin Pakistan. In Annual Technical Conference (ATC) (pp. 1-23).
- Lancaster, S., and Whitcombe, D. (2000). Fast-track 'coloured' inversion. In SEG Technical Program Expanded Abstracts 2000 (pp. 1572-1575). Society of Exploration Geophysicists.
- Langlais, V., Le Ravalec, M., & Lucet, N. (2008). U.S. Patent No. 7,400,978. Washington, DC: U.S. Patent and Trademark Office.

- Lloyd, H. J., and Margrave, G. F. (2011). Bandlimited impedance inversion: using well logs to fill low frequency information in a non-homogenous model. CREWES Research Report, No. 23.
- Lucia, F. J. (1995). Rock-fabric/petrophysical classification of carbonate pore space for reservoir characterization. AAPG bulletin, 79(9), 1275-1300.
- Maulana, T. (2016). Quantitative Seismic Interpretation using Rock Physics Templates-case examples from the Zumba field (Master's thesis, NTNU).
- Maurya, S. P. and Singh, K. (2015a). Band-limited impedance inversion of blackfoot field alberta, canada. In 37th Annual Convention Seminar and Exhibition on Exploration Geophysics.
- Maurya, S. and Singh, K. (2015b). Reservoir characterization using model based inversion and probabilistic neural network. In 1st international conference on Recent trend in engineering and Technology
- Maurya, S. P., and Sarkar, P. (2016). Comparison of Post stack Seismic Inversion Methods: A case study from Blackfoot Field, Canada. International Journal of Scientific and Engineering Research, 7 (8), 1091-1101.
- Mukerji, T., Avseth, P., Mavko, G., Takahashi, I., & González, E. F. (2001). Statistical rock physics: Combining rock physics, information theory, and geostatistics to reduce uncertainty in seismic reservoir characterization. The Leading Edge, 20(3), 313-319.
- Naseer, M. T., & Asim, S. (2017). Continuous wavelet transforms of spectral decomposition analyses for fluvial reservoir characterization of Miano Gas Field, Indus Platform, Pakistan. Arabian Journal of Geosciences, 10, 1-20.
- Pluijm, B., and Marshak, S. (2004). Earth Structure.
- Quadri, V. N., and Quadri, S. M. G. J. (1998). Cretaceous of Pakistan, India should hold more promise. Oil and Gas Journal, 96(28), 85-88.
- Russell, B., and Hampson, D. (1991). Comparison of poststack seismic inversion methods. In SEG Technical Program Expanded Abstracts 1991 (pp. 876-878). Society of Exploration Geophysicists.
- Schön, J. H., and Schön, S. J. (2011). Handbook of petroleum exploration and production.
- Smewing, J. D., Warburton, J., Daley, T., Copestake, P., and Ul-Haq, N. (2002). Sequence stratigraphy of the southern Kirthar fold belt and middle Indus basin, Pakistan. Geological Society, London, Special Publications, 195(1), 273-299.
- Talib, M., Durrani, M. Z. A., Palekar, A. H., Sarosh, B., & Rahman, S. A. (2022). Quantitative characterization of unconventional (tight) hydrocarbon reservoir by integrating rock physics analysis and seismic inversion: a case study from the Lower Indus Basin of Pakistan. Acta Geophysica, 70(6), 2715-2731.
- Telford, W. M., Geldart, L. P., Sheriff, R. E., and Keys, D. A., 1976, Applied geophysics.
- Tittman, J., & Wahl, J. S. (1965). The physical foundations of formation density logging (gamma-gamma). Geophysics, 30(2), 284-294.
- Toosy, M., Khan, S., Shakir, U., Nisar, U. B., Ullah, K., Qadir, A., & Siddique, M. (2021). Depositional architecture of Eocene and Cretaceous reservoirs (blending seismic and well data) in Mubarik Area, Central Indus Basin, Pakistan. Pure and Applied Geophysics, 178, 1297-1315.
- Veeken, P. C. H., and Da Silva, A. M. (2004). Seismic inversion methods and some of their constraints. First break, 22(6), 47-70.
- Walls, J., Dvorkin, J., and Carr, M. (2004, January). Well logs and rock physics in seismic reservoir characterization. In Offshore technology conference. Offshore Technology Conference.
- Wang, Y. (2003). Seismic amplitude inversion in reflection tomography (Vol. 33). Elsevier.
- Waters, K. (1987). Reection seismology, a tool for energy resource exploration.
- wiki.aapg.org/Seismic_inversion
- Xie, X. B., Wu, R. S., Fehler, M., and Huang, L. (2005). Seismic resolution and illumination: A wave-equation-based analysis. In SEG technical program expanded abstracts 2005 (pp. 1862-1865). Society of Exploration Geophysicists.
- Zareef, F., Khan, N., Asim, S., & Naseer, M. T. (2016). 2D seismic reservoir characterization of the Lower Goru Formation, Miano gas field, Lower Indus Basin, Pakistan. Journal of Himalayan Earth Science, 49(2).